

THE STRATIGRAPHIC EVOLUTION OF ONLAP IN SILICICLASTIC DEEP-WATER SYSTEMS: AUTOGENIC MODULATION OF ALLOGENIC SIGNALS

EUAN L. SOUTTER, IAN A. KANE, ARNE FUHRMANN, ZOË A. CUMBERPATCH, AND MADRS HUUSE
Department of Earth and Environmental Sciences, University of Manchester, Oxford Road, Manchester M13 9PL, U.K.
e-mail: euan.soutter@manchester.ac.uk

ABSTRACT: Seafloor topography affects the sediment gravity flows that interact with it. Understanding this interaction is critical for accurate predictions of sediment distribution and paleogeographic or structural reconstructions of deep-water basins. The effects of seafloor topography can be seen from the bed scale, through facies transitions toward intra-basinal slopes, to the basin scale, where onlap patterns reveal the spatial evolution of deep-water systems. Basin-margin onlap patterns are typically attributed to allogenic factors, such as sediment supply signals or subsidence rates, with few studies emphasizing the importance of predictable spatio-temporal autogenic flow evolution. This study aims to assess the autogenic controls on onlap by documenting onlap styles in the confined Eocene-to-Oligocene deep-marine Annot Basin of SE France. Measured sections, coupled with architectural observations, mapping, and paleogeographical interpretations, are used to categorize onlap styles and place them within a generic stratigraphic model. These observations are compared with a simple numerical model. The integrated stratigraphic model predicts that during progradation of a deep-water system into a confined basin successive onlap terminations will be partially controlled by the effect of increasing flow concentration. Initially thin-bedded low-density turbidites of the distal lobe fringe are deposited and drape basinal topography. As the system progrades these beds become overlain by hybrid beds and other deposits of higher-concentration flows developed in the proximal lobe fringe. This transition is therefore marked by intra-formational onlap against the underlying and lower-concentration lobe fringe that drapes the topography. Continued progradation results in deposition of lower-concentration deposits in the lobe off-axis, resulting in either further intra-formational onlap against the lobe fringe or onlap directly against the hemipelagic basin margin. Basinal relief is gradually reduced as axial and higher-volume flows become more prevalent during progradation, causing the basin to become a bypass zone for sediment routed down-dip. This study presents an autogenic mechanism for generating complex onlap trends without the need to invoke allogenic processes. This has implications for sequence-stratigraphic interpretations, basin subsidence history, and forward modeling of confined deep-water basins.

INTRODUCTION

Deep-water lobes are amongst the largest sedimentary bodies on Earth and comprise terrigenous sediment shed from the adjacent continental shelf and slope (e.g., Piper et al. 1999; Talling et al. 2007; Pr lat et al. 2010; Clare et al. 2014). They offer a record of Earth's climate and sediment transport history, form valuable hydrocarbon reservoirs, aquifers, and are sites of mineral accumulation (e.g., Weimer and Link 1991; Hodgson 2009; S mme et al. 2011; Bell et al. 2018a). Sediment-gravity-flow evolution across unconfined deep-water settings results in a fairly uniform radial spreading and deceleration of flows, and development of elongate to lobate sedimentary bodies with predictable facies transitions (e.g., Baas 2004; Hodgson et al. 2009; Spychala et al. 2017).

Sediment gravity flows encountering seafloor topography in confined-basin settings form a range of onlap geometries that are often associated with complicated sedimentary facies (Fig. 1) (e.g., Kneller 1991; Haughton 1994; Wynn et al. 2000; McCaffrey and Kneller 2001; Amy et al. 2004; Gervais et al. 2004; Lomas and Joseph 2004; Puigdef bregas et al. 2004; Smith 2004a, 2004b; Smith and Joseph 2004; Gardiner 2006; Mayall et al. 2010; Tinterri et al. 2016; Hansen et al. 2019). The effect of seafloor

topography on sediment gravity flows, their deposits, and onlap styles has been studied through outcrop data (e.g., Kneller et al. 1991; Sinclair 1994; Bakke et al. 2013), subsurface data (e.g., Prather et al. 1998, 2012; Covault and Romans 2009; Bakke et al. 2013), and numerical models (e.g., Smith 2004b; Kubo 2004; Gardiner 2006; Sylvester et al. 2015) and physical models (e.g., Kneller 1995; Kneller and McCaffrey, 1995; Amy et al. 2004; Brunt et al. 2004; Kubo 2004). Seafloor topography is generated by a variety of geological processes, such as: pre-depositional tectonic deformation (e.g., Jackson et al. 2008; Kilhams et al. 2012), syn-depositional tectonic deformation (e.g., Wilson et al. 1992; Haughton 2000; Grecula et al. 2003; Hodgson and Haughton 2004; Tomasso and Sinclair 2004; Kane et al. 2010; Salles et al. 2014), mass transport deposit relief (e.g., Armitage et al. 2009; Ortiz-Karpf et al. 2015, 2016; Kneller et al. 2016; Soutter et al. 2018) and salt diapirism (e.g., Hodgson et al. 1992; Kane et al. 2012; Prather et al. 2012; Oluboyo et al. 2014; Doughty-Jones et al. 2017). Improved prediction of the distribution of sediment gravity flow deposits around seafloor topography is therefore critical for both paleogeographic reconstructions (e.g., Pinter et al. 2017) and stratigraphic hydrocarbon or CO₂ trap risking (e.g., McCaffrey and Kneller 2001).

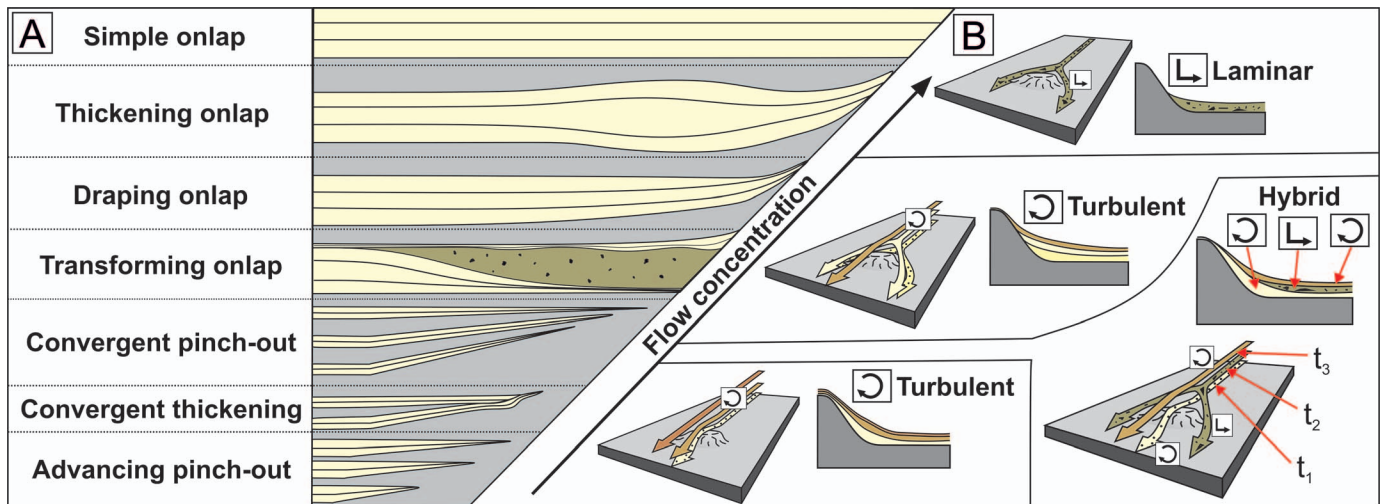


Fig. 1.—**A**) Examples of onlap termination styles (modified from Al Ja'aidi et al. 2004; Bakke et al. 2013; Patacci et al. 2014). **B**) Generalized relationship between flow concentration and onlap geometry (modified from Bakke et al. 2013). t , time.

The onlap geometry (3D shape of an event bed or sequence of related event beds at pinch-out) and facies (internal sedimentary characteristics of an event bed at pinch-out) (Fig. 1A), herein termed onlap termination, are controlled by: 1) flow magnitude, duration, velocity, thickness, concentration, and sediment composition; 2) the gradient and incidence angle of the counter-slope; and 3) seafloor composition and induration. Typically, high-concentration flows and steep counter-slopes cause abrupt terminations, whereas low-concentration flows and shallow counter-slopes cause draped terminations (Fig. 1) (Smith and Joseph 2004; Bakke et al. 2013). Flows with a high mud content may also be more prone to varying degrees of rheological transformation approaching counter-slopes, resulting in complicated facies distributions at confining basin margins (Fig. 1) (Barker et al. 2008; Patacci et al. 2014; Southern et al. 2015).

Recent field-based studies on the spatial and temporal evolution of unconfined submarine lobes have used the longitudinal evolution of flows and their associated facies to establish criteria for differentiating lobe sub-environments at the bed scale (e.g., Prélat et al. 2009; Grundvag et al. 2014; Sychala et al. 2017). The applicability of these facies associations to confined lobes and the complex system-scale stacking patterns that they may produce is only recently being investigated (e.g., Marini et al. 2015; Sychala et al. 2015, 2017; Bell et al. 2018b; Fonnesu et al. 2018; Liu et al. 2018). Previous flow-dependant onlap models mainly focused on end-member geometries (e.g., McCaffrey and Kneller 2001; Smith 2004b; Smith and Joseph 2004). As yet there is no generic model to account for how the wide variety of deposits resulting from the longitudinal evolution of sediment gravity flows will manifest themselves at onlap surfaces through the fill of a confined basin.

This study uses the well-constrained Cenozoic Annot Basin of SE France to integrate bed-scale and basin-scale onlap observations into a generically applicable depositional model. The aims of this study are to: i) reappraise the Annot Basin stratigraphy with respect to specific deep-water sub-environments, with particular emphasis on the poorly studied eastern exposures of the basin, ii) document lateral facies changes within beds approaching the basin margin and relate these facies changes to longitudinal flow evolution, iii) assess how the longitudinal evolution of confined flows impacts onlap geometry and stacking patterns, and iv) integrate these observations into a generic model for the evolution of onlap in deep-water basins.

THE ANNOT BASIN

Basin Structure

The 160-km-long and 80-km-wide (Clark and Stanbrook 2001) Cenozoic foreland basin of the western Alps formed due to SW-directed collision of the Adria and European plates, and subsequent loading of the European plate by the Alpine orogenic wedge (Figs. 2, 3) (e.g., Ford et al. 1999). This orogenic deformation is represented in the foreland-basin stratigraphy by a progressive younging to the southwest (e.g., Ford et al. 1999; Du Fornel et al. 2004). Sediment deposition in the basin was affected by complicated basinal topography (e.g., Joseph and Lomas 2004), which formed due to Late Cretaceous northward-directed Pyrenean compression that was subsequently overprinted by Cenozoic SW-directed Alpine compression (Fig. 3) (e.g., Apps et al. 2004). This resulted in NW–SE-oriented synclinal sub-basins with E–W anticlinal sills. The synclines are interpreted as the surface expression of underlying Alpine thrust-fault-propagation anticlines (Fig. 3) (e.g., Elliott et al. 1985; Apps 1987; Ravenne et al. 1987).

The Annot sub-basin, herein termed the Annot Basin, is one of the exhumed synclinal Cenozoic depocenters in the Alpine foreland basin, representing the proximal end of the deep-marine Annot–Grand Coyer–Chalufy chain of sub-basins (Figs. 2, 3) (see Joseph and Lomas 2004, for review). The Annot Basin is bounded to the south by the SW–NE Rouaine Fault Zone, which acted as an entry point for sediment gravity flows into the basin (e.g., Salles et al. 2014) (Figs. 2, 3). The SW–NE Braux normal fault is related to this fault zone and created local bathymetric relief during the late Eocene (e.g., Tomasso and Sinclair 2004) (Figs 3, 4). The western and eastern margins of the basin are defined by fault-propagation anticlines created by Mesozoic blind thrusts (Figs. 3, 4) (e.g., Apps 1987). The eastern margin is formed by the Melina anticline, or “kink zone” (Apps 1987), and the western margin by the Puy du Rent anticline (Fig. 3; 4B). These anticlines were developing during deposition of the Annot turbidites, causing syn-depositional rotation of the basin depocenter towards the west (Fig. 3) (e.g., Salles et al. 2014).

E–W-oriented Pyreneo-Provençal structures also affect the Annot Basin structure, with the northern extent of the basin formed by the Aurent anticline (Fig. 3). This structure forms a gently southward-dipping terminal slope (e.g., McCaffrey and Kneller 2004). More minor basin-floor relief may have been formed by the E–W Fugeret anticline, which lies between the Rouaine fault zone and the Aurent anticline (Fig. 3) (Salles et al. 2014). These E–W-oriented structures show little evidence of major syn-

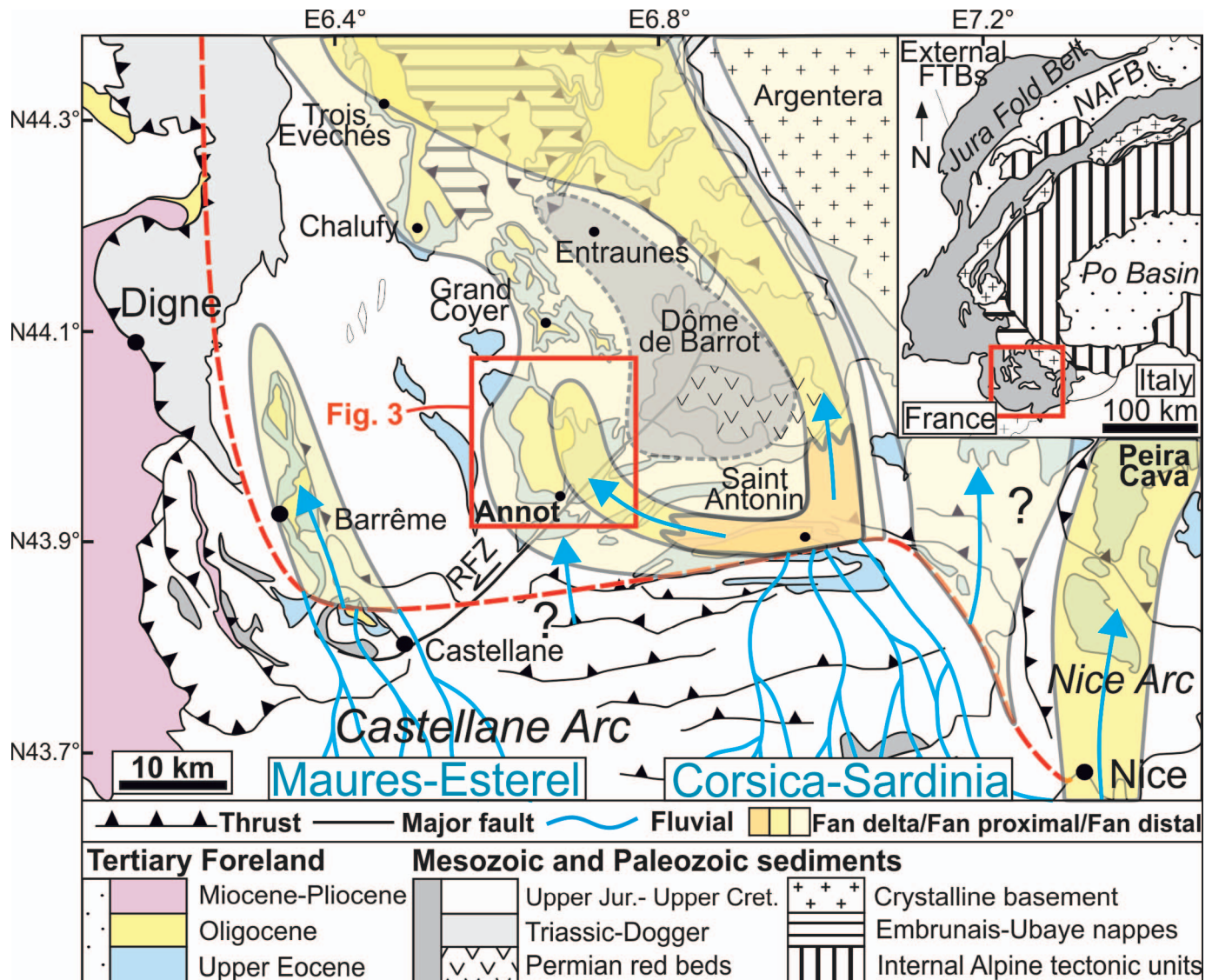


Fig. 2.—Location and geological setting of the Cenozoic foreland basin of the Western Alps. The generalized late Eocene paleogeography is overlaid (modified from Joseph and Lomas 2004 and Salles et al. 2014) and shows the Annot Basin (red box) situated in a clastic deep-marine environment. Red line indicates boundary between terrestrial and marine environments. RFZ, Rouaine Fault Zone. Blue arrows indicate paleoflow, and blue lines indicate schematic fluvial systems.

depositional movement due to compressional deformation being dominantly driven by the SW-directed Alpine orogeny during the Eocene and Oligocene.

Stratigraphic Evolution

The Annot Basin has the same transgressive Cenozoic foreland-basin stratigraphy as is seen across the western Alps (Figs. 2, 3) (e.g., Sinclair 1997), with Oligocene shallow-marine limestones of the Calcaires Nummulitique overlain by deep-marine marls of the Marnes Bleues. The Marnes Bleues records the deepening of the basin, with foraminifera suggesting water depths of ~100 m at the base of the succession, to ~800 m by the end of deposition (Mougin 1978). Supply of siliciclastic sediment began abruptly in the late Eocene (35.2 Ma) as the Corsica–Sardinia massifs were uplifted via subduction-related back-thrusting to the south (Fig. 2) (e.g., Stanley and Mutti 1968; Apps 1987). This resulted in a depositional shift from the marls of the underlying Marnes Bleues, into south-to-north dispersing clastic sediment gravity flows of the Grès d’Annot. An upwards coarsening trend in the Grès d’Annot suggests

progradation of the clastic system, most-likely related to fan-delta advance (Fig. 3) (e.g., Puigdefàbregas et al. 2004).

During early clastic deposition the Annot Basin was located on the western side of a distal submarine fan extending over the foreland basin, with flows entering the basin from syncline-bounded fan deltas to the south (Fig. 2) (e.g., Stanley 1980; Sinclair 2000; Joseph and Lomas 2004) and being dispersed northwards through relay ramps in the Rouaine Fault Zone (Fig. 3) (Joseph and Lomas 2004; Salles et al. 2014). This early deposition is represented in the Annot Basin by low-density turbidites, often referred to as the Marnes Brunes Inferièures (e.g., Stanbrook and Clark 2004), which form the distal equivalent of the Grès d’Annot. The lowermost Grès d’Annot member, termed Le Ray (Puigdefàbregas 2004) or the A Member (Du Fournel et al. 2004), onlaps both the underlying Marnes Brunes and Marnes Bleues slope (Fig. 3). Early flows were confined by the Braux Fault to the west, a combination of the Braux Fault and the Fugeret anticline to the north, and the Melina anticline to the northeast (Salles et al. 2014). The sediment entry point shifted throughout deposition of the Grès d’Annot, with a more easterly late Eocene entry point suggested for these early

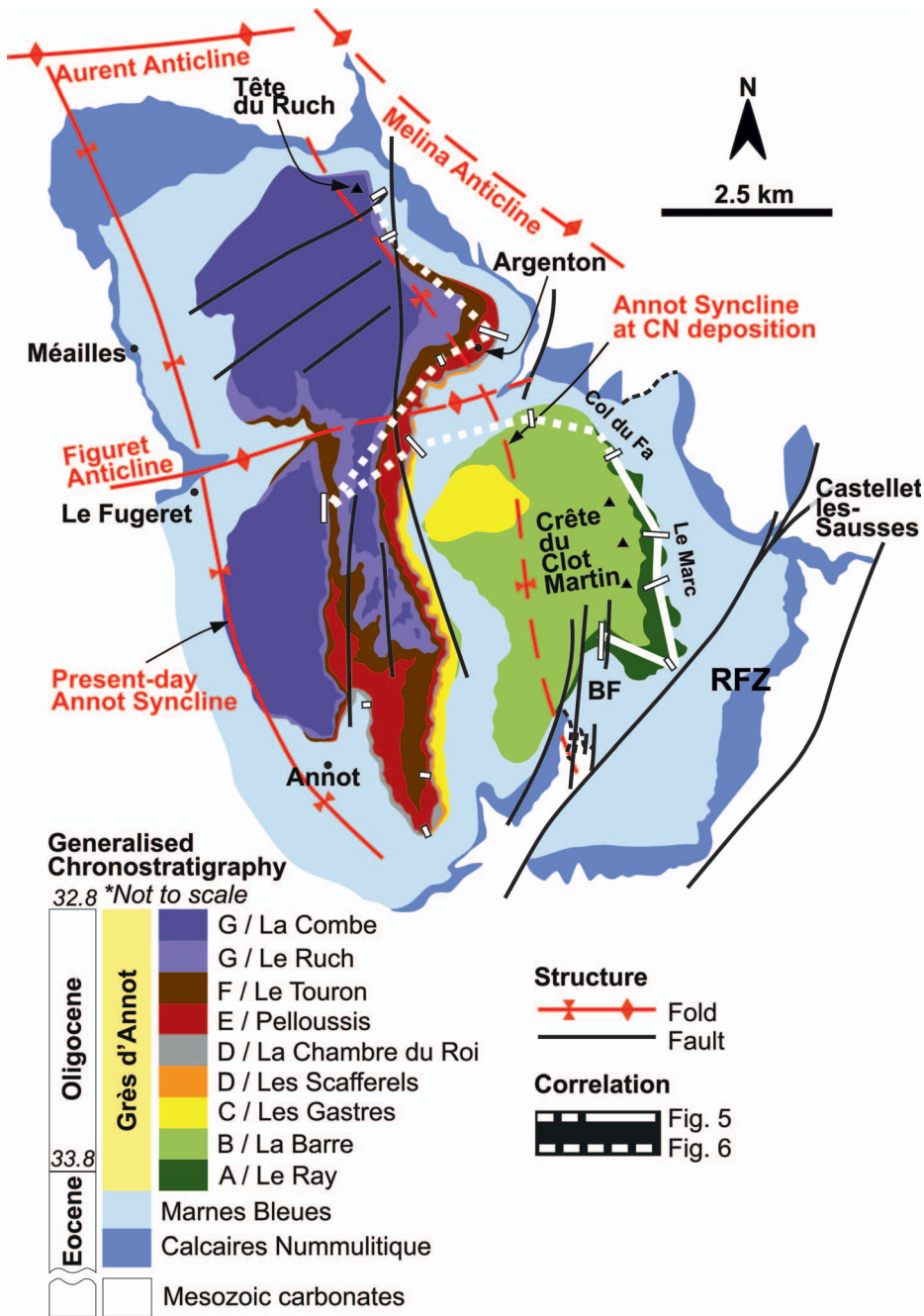


FIG. 3.—Structure, chronostratigraphy, and geological map of the Annot Basin (modified from Puigdefàbregas et al. 2004; Du Fornel et al. 2004; Salles et al. 2014). The various anticlines confine deposition across the Basin. The clastic sequence has been divided into members based on aerial and outcrop mapping (modified from Puigdefàbregas et al. 2004; Salles et al. 2014). An attempt has been made to reconcile the member subdivisions used by Puigdefàbregas et al. (2004) and Salles et al. (2014). White boxes indicate logged localities. White lines indicate correlation panels in Figures 5 and 6. RFZ, Rouaine Fault Zone; BF, Braux Fault. Black dashed lines indicate exhumed syn-sedimentary fault escarpments.

flows, as evidenced by an up-stratigraphy rotation of paleocurrents from NE- to NW-directed (McCaffrey and Kneller 2004; Salles et al. 2014). Alternatively, this may be an apparent repositioning of the sediment entry point as the basin depocenter itself migrated gradually westward due to Alpine compression (Salles et al. 2011, 2014). This deformation is believed to have been continuous throughout the fill of the basin; however, the apparent rate of deformation is suppressed in the Grès d'Annot due to the higher depositional rates associated with gravity-flow deposition (Apps et al. 2004). The remaining Grès d'Annot members were confined by the major Melina (east), Puy du Rent (west), and Aurent anticlines (north) as the topography of the Braux Fault and Fugeret Anticline was healed relatively early in the Oligocene (Fig. 3) (Salles et al. 2014).

The basin gradually filled throughout the early Oligocene, with contemporaneous deposition occurring in the parallel Grand Coyer sub-

basin to the northeast (Salles et al. 2014). Once the basin was largely filled, the Aurent Anticline ceased to terminally confine flows, and flows bypassed the Annot Basin into the Grand Coyer and Chalufy sub-basins (Fig. 2) (e.g., Apps 2004; Salles et al. 2014). Few channel fills are seen within the Grès d'Annot succession, and the depositional architecture is interpreted as being predominantly sheet-like (Apps 1987).

DATA AND METHODS

The dataset comprises 50 (581 m cumulatively) sedimentary logs collected along sections predominantly oriented oblique to depositional-dip along the eastern margin of the Annot Basin (Figs. 3, 4A, 5). Logs were collected at 1:10 scale, and individual beds were walked out at outcrop (Figs. 6, 7). Higher resolution 1:2 scale logs were collected from some

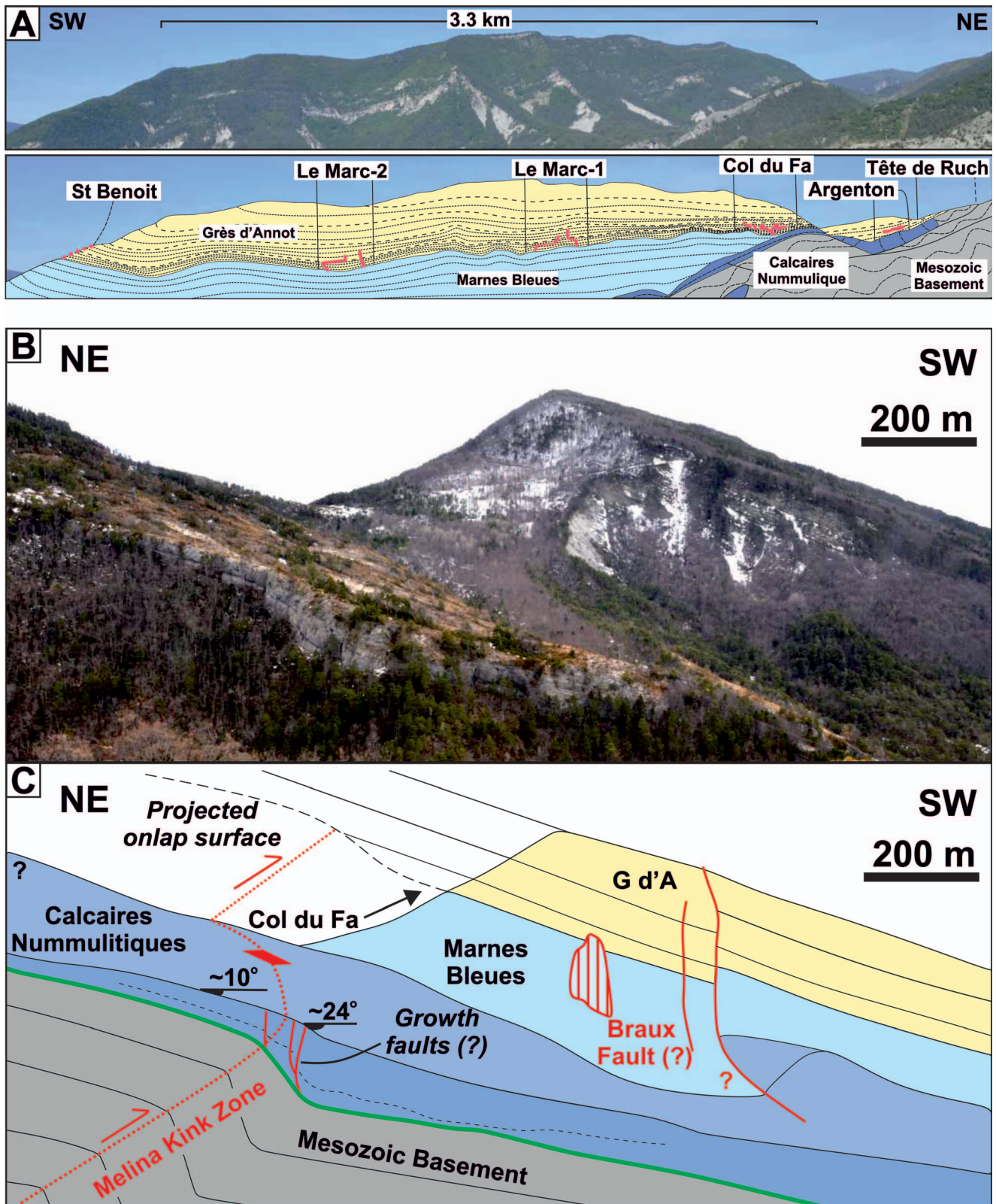


FIG. 4.—A) Dip and B) strike field sketches of the stratigraphy and structure of the Annot Basin. Logged localities are shown as red traverses in Part A.

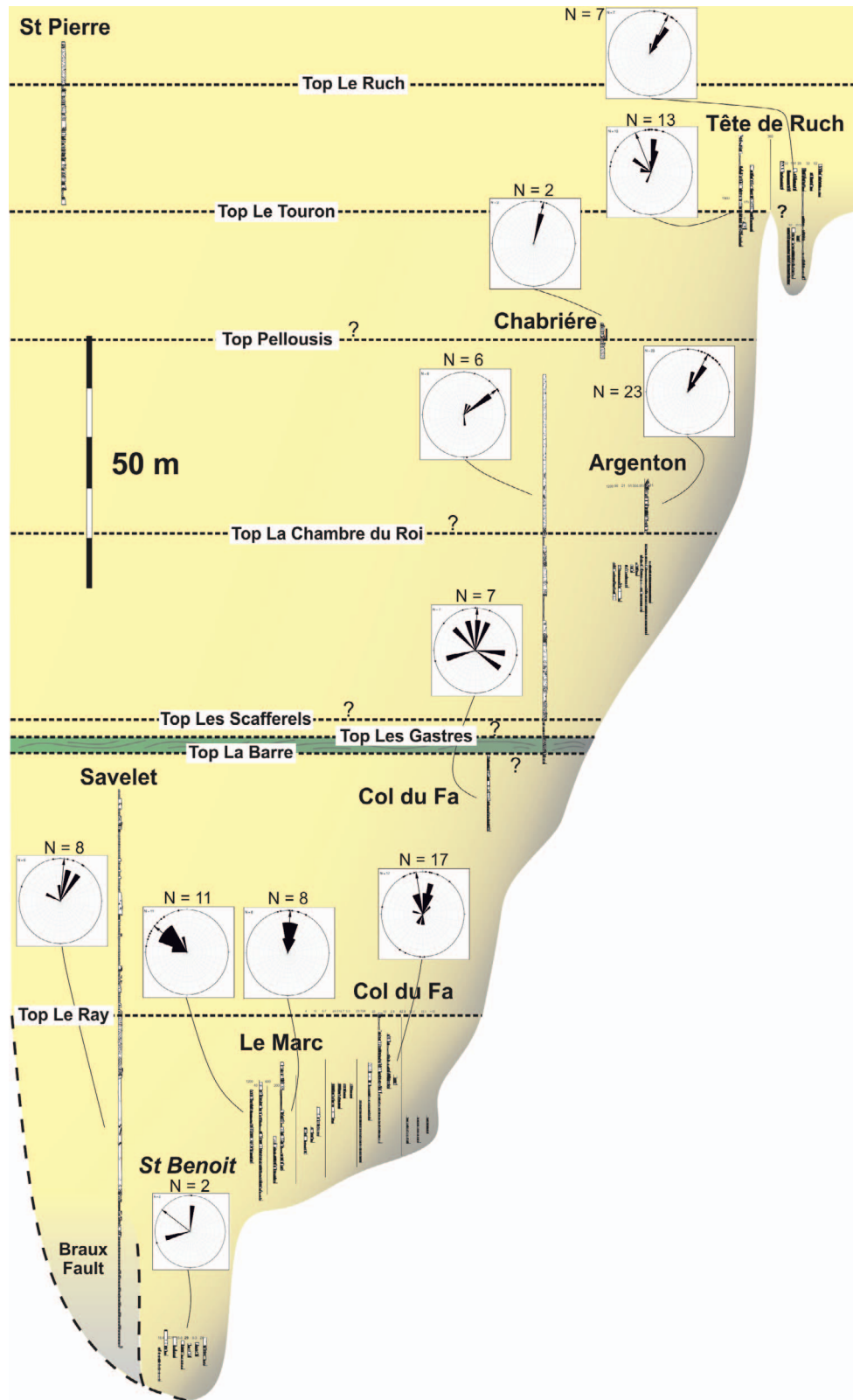


FIG. 5.—Dip-oblique correlation panel along the eastern margin of the Annot Basin. No horizontal scale. Localities and panel orientation are shown in Figure 3. Members have been correlated based on published maps and lithological observations. Paleocurrent data are associated with one sedimentary log or series of logs from one locality. The vertical thickness represents the exposed stratigraphy along the correlated margin (see Fig. 3 for location) and does not represent the accommodation of the entire basin, which had a westward-migrating depocenter. This migration is represented in the eastern exposures by decreasing member thicknesses through time. It should also be noted that due to the oblique nature of the correlation the margin position is a representation of the relative confinement on a member scale and does not indicate onlap angle.

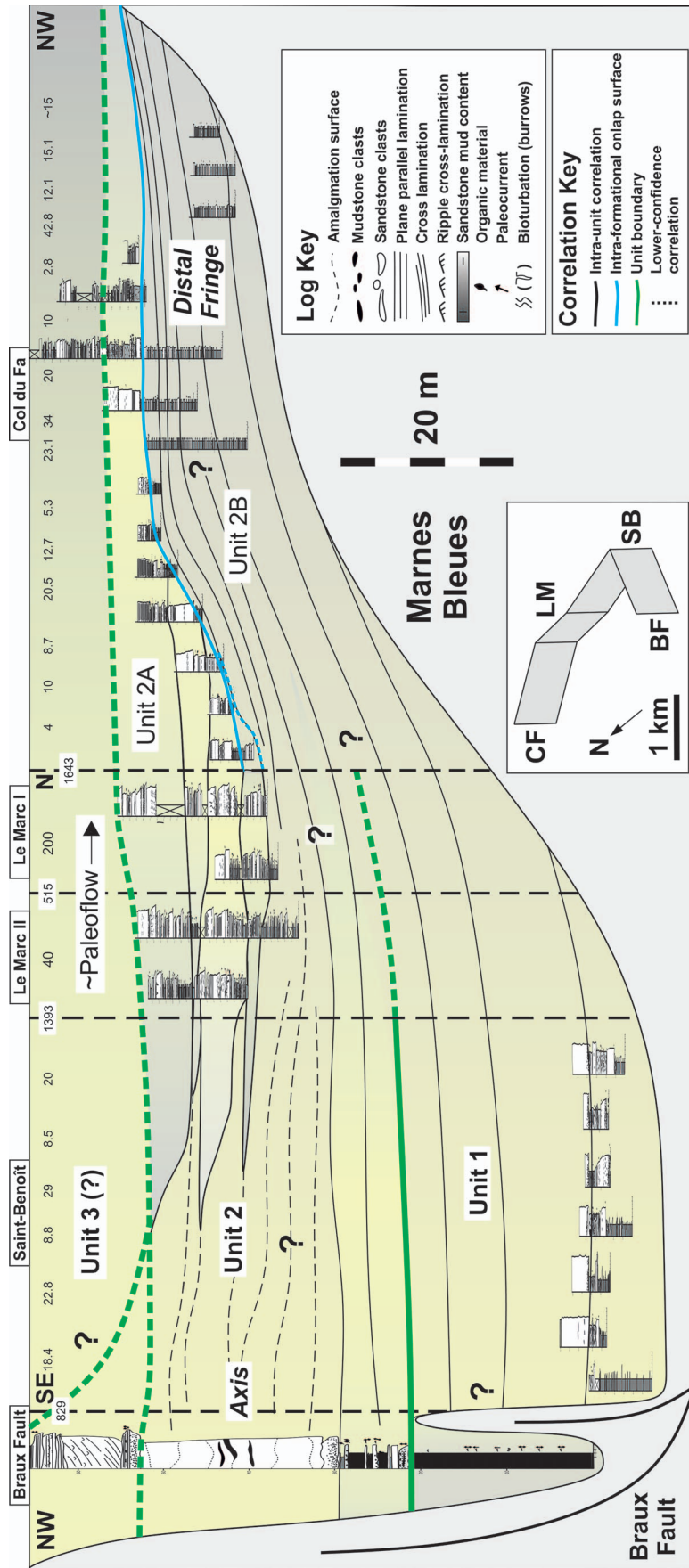


FIG. 6.—Correlation panel for the Le Ray member in the Annot Basin. Paleoflow is from the left to right (south to north). Inset shows 3D orientation of panel. BF, Braux Fault; SB, Saint-Benoit; LM, Le Marc; CF, Col du Fa.

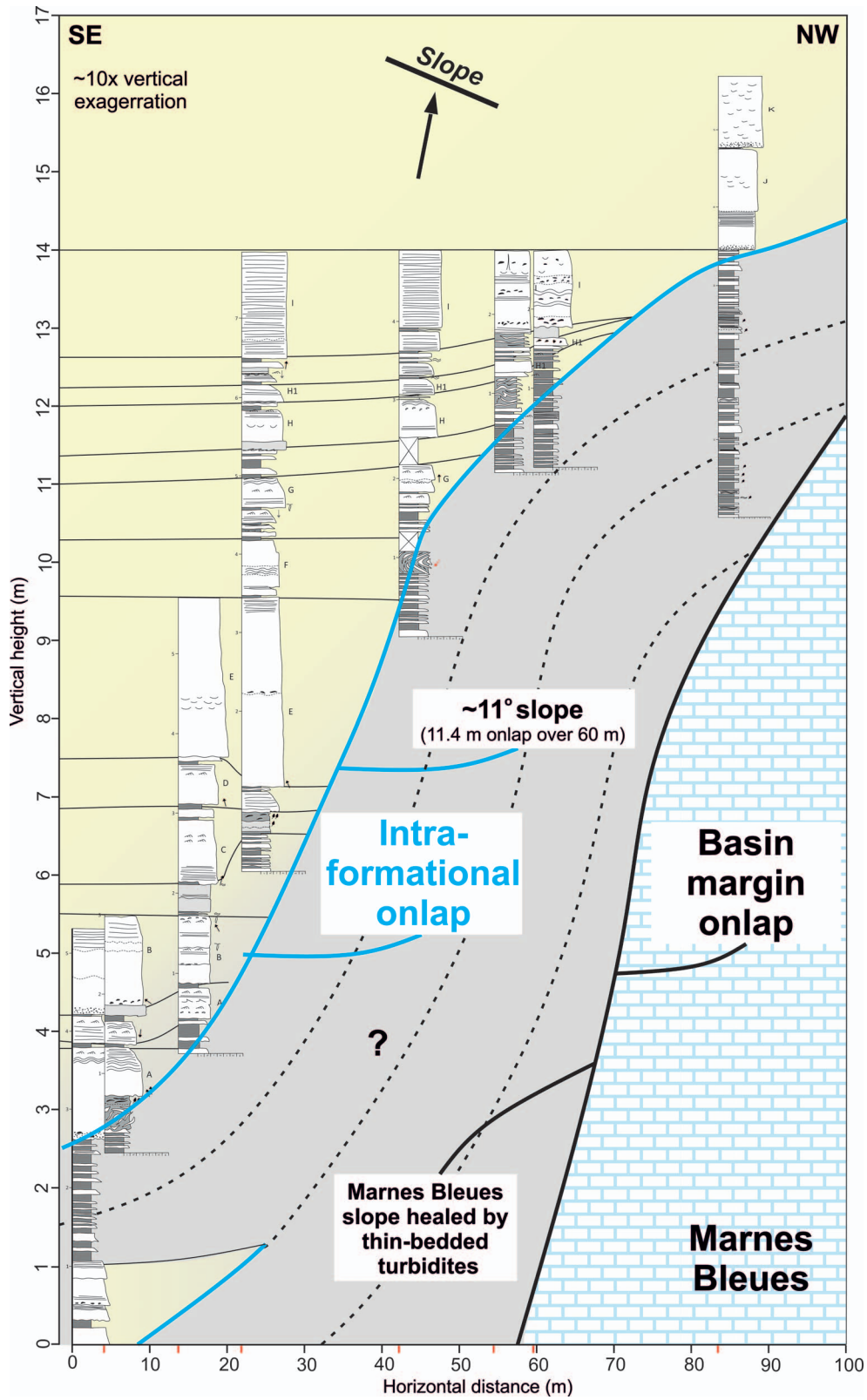


FIG. 7.—Correlation panel from the Col du Fa outcrop. The thinner-bedded low-density turbidites drape and heal the topography of the Marnes Bleues basin margin onlap surface, while the higher-density and thicker-bedded turbidites initially onlap against these distal deposits, forming an intra-formational onlap surface. Red lines on the horizontal axis indicate exact log position. Log key in Figure 6.

TABLE 1.—Key lithofacies, facies associations, and onlap geometries seen in the Grès d'Annot of the Annot Basin.

Lithofacies	Description	Interpretation	Facies Association	Onlap Geometry
Thick-bedded sandstone (LF 1)	Forms 1–20 m amalgamated packages or 0.5–2 m beds. Medium–granule grain size. Flat or erosional bed bases and flat bed tops. Mostly structureless with some planar laminae. Often contains mud clasts (< 5 cm) and soft-sediment deformation, e.g. flames and dishes.	Rapid aggradation beneath a highly concentrated flow. Planar-spaced laminae indicate traction-carpet deposition (<i>sensu</i> Lowe 1982).	Lobe axis (FA 1) Lobe off-axis	Abrupt termination High-density flows deposit abruptly at counter-slope due to loss of capacity, compared to lower-concentration flows with otherwise similar flow properties (e.g., Hiscott 1994). The slope may be draped by deposition from the overriding and dilute tail of the same flow.
Medium-bedded sandstone (LF 2)	0.1–0.8 m beds. Fine–coarse grain size. Flat or weakly erosional bed bases and flat or convolute bed tops. Flutes and grooves on bed bases. Sporadic granules sometimes present and associated with structureless lower bed divisions. Mostly normally graded with planar and convolute laminae. Ripples at bed tops.	Presence of flutes, normal grading, and tractional structures indicates deposition from a dilute turbidity current. These beds are interpreted as medium-density turbidites due to their often structureless basal divisions and thicknesses greater than 10 cm.	Lobe off-axis (FA 2) Lobe axis Proximal fringe	Abrupt to draped termination More capable of surmounting topography than higher-density flows because they are more able to maintain turbulent energy while flowing up the counter-slope (e.g., Bakke et al. 2013; Eggenhuisen et al. 2017). Wide variety of sediment concentrations in these flows causes drape to extend from meters to tens of meters up the slope.
Hybrid beds (LF 3)	0.1–1.2 m bipartite or tripartite beds. Lower medium–coarse sandstones (division 1) overlain sharply or loaded by argillaceous sandstones (division 2). Argillaceous sandstones often have a sheared fabric. Cleaner, often finer, and tractionally reworked sandstone sometimes present capping these divisions with a sharp or founded base (division 3). Decimeter scale organic material sometimes present in middle division.	Beds containing deposits of both turbulent and transitional/laminar flows interpreted as hybrid beds (<i>sensu</i> Haughton et al. 2009). Flow transformation occurs through increasing concentration of fines during run-out (e.g., Kane et al. 2017) or through forced deceleration (Barker et al. 2008; Patacci et al. 2014).	Proximal fringe (FA 3) Lobe off-axis Distal fringe Lobe axis	Abrupt to draped termination Debritic or argillaceous middle divisions are highly concentrated so terminate abruptly. Draping of the middle division may occur if the slope is shallow enough to allow run-up of the debritic middle division. The turbulent lower part of the flow may drape the slope and amalgamate with the overlying sandstone or deposit abruptly if high-density.
Thin-bedded sandstone (LF 4)	0.01–0.1 m siltstones and fine sandstones. Parallel and convolute laminae, normal grading. Flutes rarely preserved. Ripples occasionally show opposing paleoflow directions.	Fine grain size, thin event beds, and abundance of tractional structures indicates that these beds were deposited by low-density/concentration turbidity current and are therefore interpreted as low-density turbidites.	Distal fringe (FA 4) Proximal fringe Lobe off-axis	Draped termination Low-concentration flows are less affected by changes in slope angle and are thus able to surmount basin topography and drape topography for substantial distances up the counter-slope (e.g., Muck and Underwood 1990). Low-density turbidites are therefore able to dominate much of the sediment thickness on the upper parts of the confining slope.

beds approaching onlap. Logs within thin-bedded facies were collected at a 1:5 scale to allow accurate representation of their thicknesses and structures. Samples of individual facies and individual beds were collected in order to quantitatively constrain lateral grain-size and matrix changes. 104 3D paleocurrent measurements were collected (Fig. 5), with 2D paleocurrent measurements qualitatively noted.

Margin Correlation

Sedimentological contacts between the discrete members of the Grès d'Annot from the geological maps of Puigdefàbregas et al. (2004), Du Fornel et al. (2004), and Salles et al. (2014) were ground-truthed and compared to observations made by this study (Fig. 3). The observations of stratigraphic contacts made during this study most closely agree with those made by Puigdefàbregas et al. (2004); therefore their geological map was used for placement of sedimentary logs within members and for the intra-member correlation of sedimentary logs (Figs. 5, 6). This allows facies transitions across the basin to be assessed both spatially and temporally. Where member

boundaries are unclear due to the resolution of the geological map the top of individual members is defined by either abrupt facies changes, commonly an abrupt coarsening and thickening of event beds, or lateral relationships and correlations (Fig. 5). An attempt has been made to reconcile the nomenclature used by Puigdefàbregas et al. (2004) and Salles et al. (2014) to enable comparisons to be made between the two (Fig. 3).

Detailed correlations of the Le Ray member are based on the identification of key surfaces, such as onlap surfaces, and walking out of individual beds (Fig. 6). Where beds could not be walked out, units were correlated based on the methodology of Prêlat et al. (2009) for the identification of the hierarchical elements that builds lobes, e.g., beds, lobe elements, and lobes.

FACIES ASSOCIATIONS

Facies associations (FA) have been interpreted based on the dominant lithofacies (LF) and depositional features of a given succession (Table 1). The dominant lithofacies has been described and interpreted in each facies

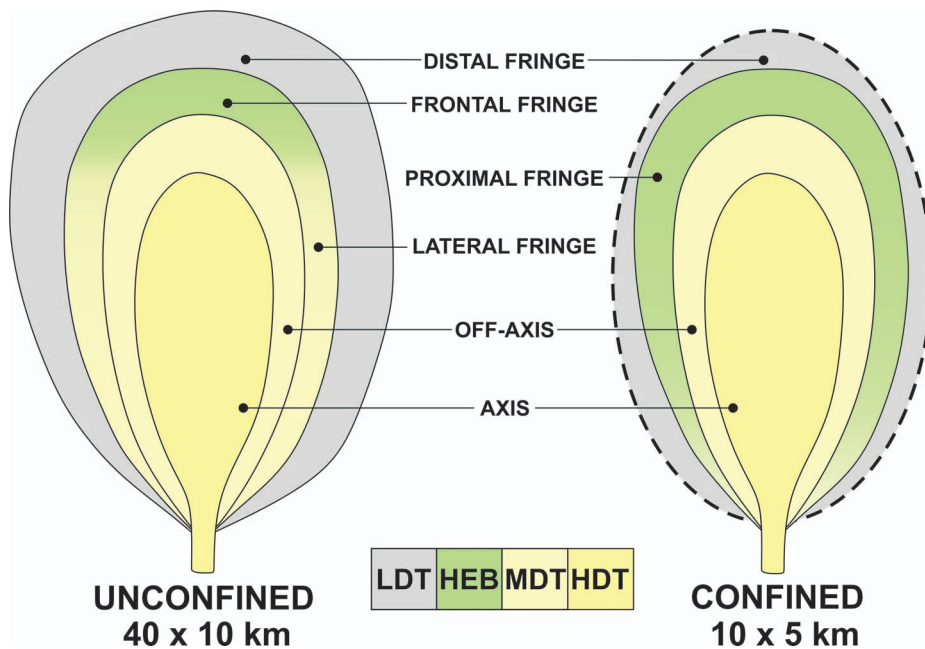


FIG. 8.—**A**) Nomenclature comparison between unconfined lobe sub-environments (Spychala et al. 2017) and **B**) confined lobe sub-environments. The only difference is that hybrid beds are more prevalent in lateral positions in confined systems due to rapid flow deceleration and transformation at basin margins. LDT, low-density turbidite; HEB, hybrid (event) bed; MDT, medium-density turbidite; HDT, high-density turbidite. Unconfined and confined lobe dimensions are from Prelat et al. (2010).

association in order to justify their placement in that sub-environment. The lobe sub-environments of Sychala et al. (2017) are used because they best fit the observations made in this study (Figs. 8, 9). The onlap geometry of each lithofacies, and therefore the inferred onlap geometry of the facies association in which that lithofacies dominantly occurs, is summarized in Table 1. Facies associations are presented in the following section from proximal to distal positions on the lobe, in descending stratigraphic order and, broadly, in descending order of thickness.

FA 1 Lobe-Axis

Observations.—Facies association 1 is composed dominantly of one lithofacies: thick-bedded (0.5–2 m) sandstones (LF 1A) (Fig. 10A, B, E) with thin-bedded (0.01–0.5 m) sandstones (LF 1B) and medium-bedded sandstones (0.1–0.8 m) (LF 3) commonly associated. LF 1B is composed of medium- to cobble-grade (most typically coarse-grained), poorly sorted, massive sandstones (Fig. 10B) and is less prevalent than LF 1A. Individual beds have erosional bases, often with groove, flute, and tool marks, and irregular tops. Beds are often lenticular, thickening and thinning from < 10 cm before pinching out over tens of meters. The beds often occur within successions of medium-bedded sandstones (LF 2) below packages of LF 1.

The thick-bedded LF 1A sandstones are medium-grained to granular sandstones with bed bases that are flat (at exposure scale) or erosional (Figs. 7, 11B). Flat bases are most prominent when overlying mudstones, while erosional bases are most commonly expressed as amalgamation surfaces (Fig. 9B, C, D). Both bedding-parallel and erosional bases are associated with decimeters of deformation in the underlying beds. This deformation obscures the primary depositional characteristics of the underlying beds, making interpretation of the deformed beds difficult. Bed bases with steeper dips than the bed top are observed at pinch-out of these beds (Fig. 11B), with bed bases steepening towards the pinch-out. Amalgamation surfaces are identified by mudstone-clast-rich rugose horizons, abrupt grain-size breaks, and truncated trace-fossil burrows. Bed tops are flat and exhibit little depositional relief. Beds are typically structureless, with rarely preserved faint parallel lamination and tractional structures, and ungraded, though some beds show weak normal grading (Figs. 7, 9B, C, D).

Interpretations.—The presence of erosional bed bases with tool marks and grooves indicates that LF 1A beds were deposited by high-concentration flows that initially carried large clasts and other detritus at the base of the flow. Superimposed flute marks, normal grading, and tractional structures are indicative of evolution to a less concentrated, more turbulent flow. The rarity of tractional structures and commonly massive and poorly sorted beds, however, indicates that these beds were deposited rapidly (*sensu* Lowe 1982). This is most likely due to a reduction in flow capacity (*sensu* Hiscott 1994), preventing the formation of grading and the preservation of bedforms. These turbidites are therefore interpreted as high-density turbidites (*sensu* Lowe 1982). The presence of deformation structures beneath these flows has been attributed to high shear stresses acting on the seabed (e.g., Clark and Stanbrook 2001; Puigdefàbregas et al. 2004). These laterally extensive (up to 1 km where outcrop allows) high-density turbidites, which are commonly amalgamated, are interpreted to be analogous to lobe axis deposits observed elsewhere (e.g., Prêlat et al. 2009).

The coarse grain size and thin-bedded nature of LF 1B suggests that these beds were deposited as a coarse-grained lag in a bypass-dominated part of the system. The lenticular geometry suggests that either i) flow energy, and therefore bypass potential, was not homogeneous laterally within the flow or ii) erosion by later flows or waxing of the flow (Kane et al. 2009), scoured the bed top (Fig. 10B). Because this lithofacies is confined stratigraphically to sequences underlying thick-bedded and amalgamated sandstones of similar grain sizes, they are inferred to be laterally related. These lags are interpreted to represent a mostly bypassing equivalent of the thick-bedded sandstones in the lobe axis.

FA 2: Lobe Off-Axis

Observations.—Facies association 2 is composed primarily of normally graded medium-bedded (0.1–0.8 m) fine- to medium-grained sandstones (LF 2) with flat to slightly erosional bed bases and flat bed tops (Figs. 7, 10A, 12). Flutes and grooves are often seen at bed bases. Ripples at bed tops commonly show opposing paleoflow directions to those measured from flutes and grooves on individual event beds (Fig. 5). Beds pinch out abruptly towards the basin margin, and often can be traced away from the onlap surface to a parent thick-bedded sandstone (Fig. 7). In the uppermost

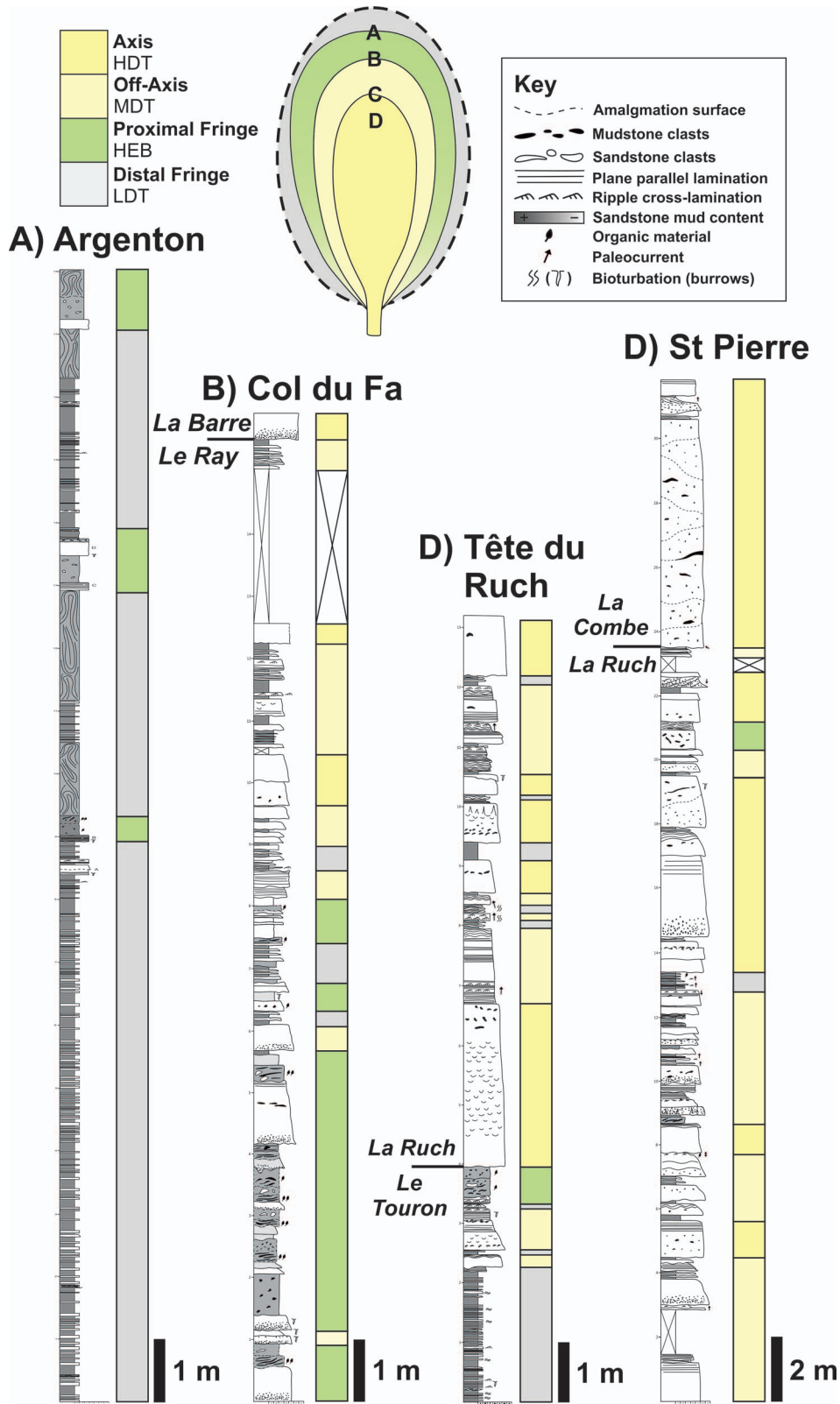


FIG. 9.—Sedimentary logs with facies and paleogeographical interpretations. Each member contains elements of each lobe sub-environment; however, there is an increasing prevalence of higher-density deposits upwards through stratigraphy. This pattern is interpreted as representing overall lobe progradation. Colored bars next to logs represent facies on sub-environment key.

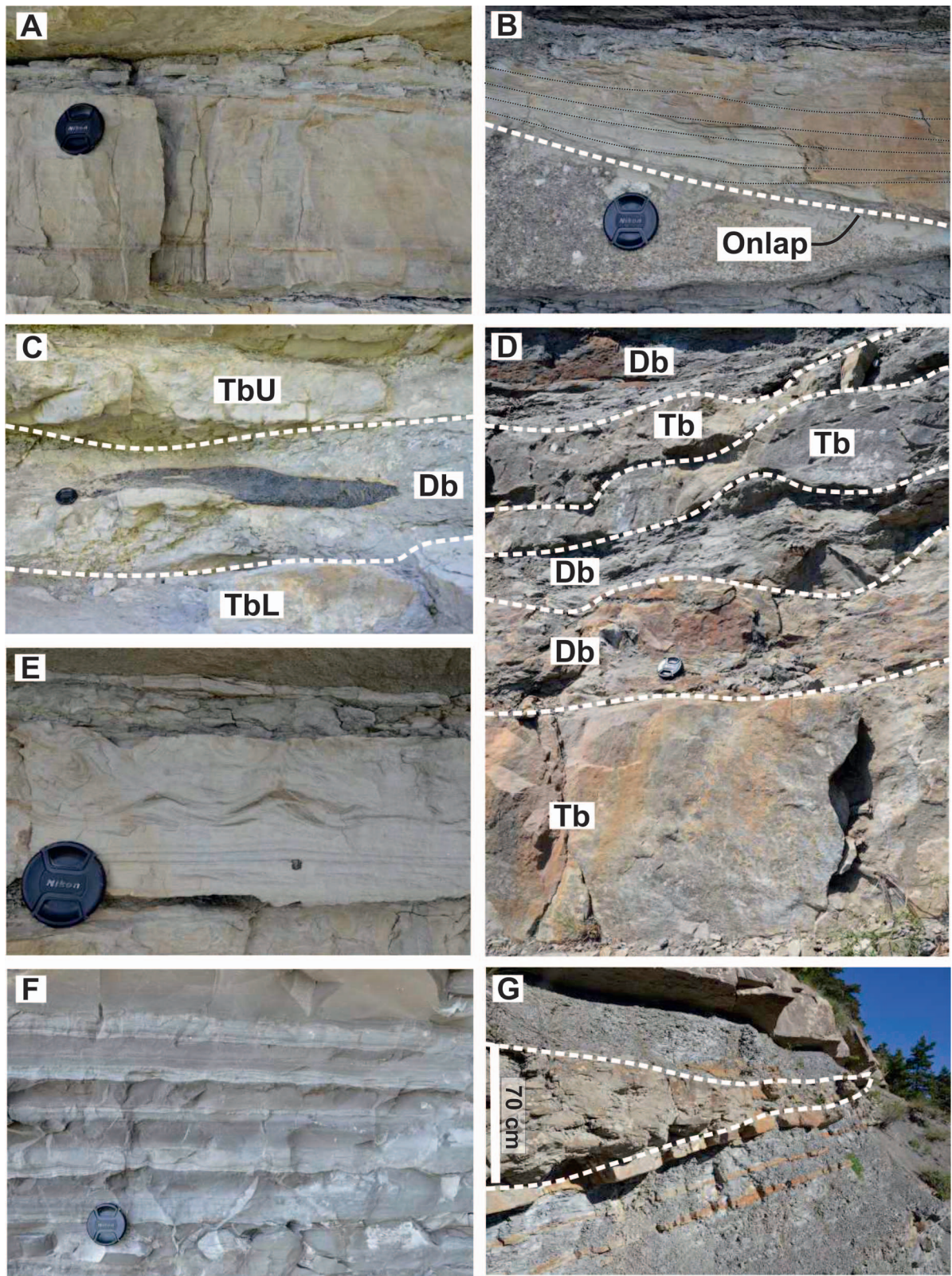


FIG. 10.—**A**) Medium-density turbidite (MDT) at Col du Fa. **B**) Low-density turbidite (LDT) onlapping a gravel lag deposit at Tête du Ruch (Lower). **C**) Organic material in the debritic division of a hybrid bed at Le Marc. **D**) Pinch-out amalgamation zone at Col du Fa. Debritic (Db) and turbiditic (Tb) sections can be identified and correlate with thick- and medium-bedded turbidites up-dip. It is difficult to differentiate groups of event-beds in these slope proximal units. **E**) Highly tractionally r-worked LDT. **F**) Typical thin-bedded LDT facies. **G**) Slumped thin-bedded turbidites at Argenton. Fold hinges indicate failure perpendicular to the slope.

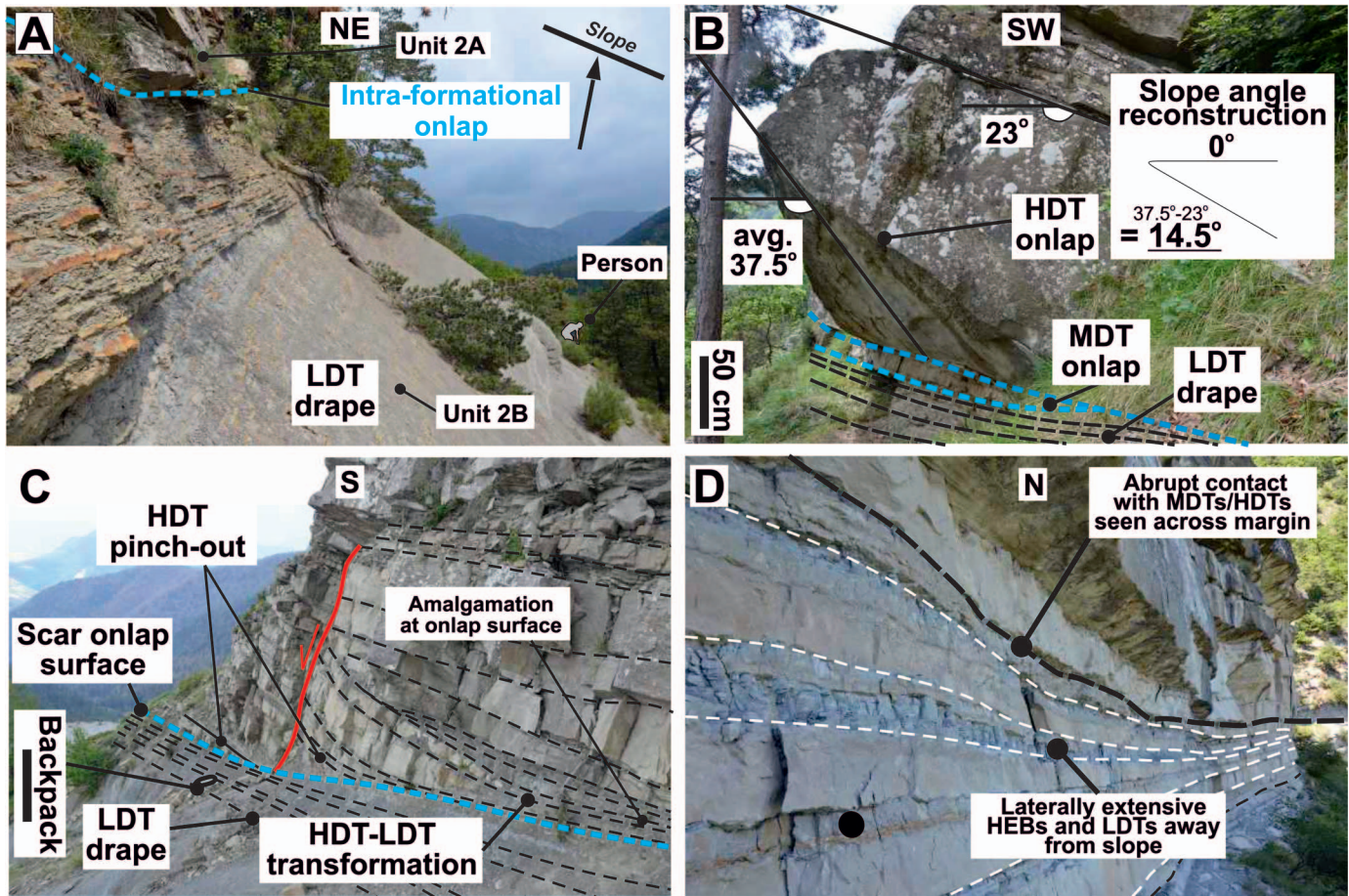


FIG. 11.—A) Contact between the thin beds and high-density turbidites at Col du Fa. The high-density turbidites onlap against the low-density turbidite slope drape at an incidence angle almost perpendicular to the slope (arrow is paleoflow). B) Example of a high-density turbidite with a wedged base onlapping the underlying slope drape. Restoring the bed top to horizontal allows a rough estimate of the paleo-slope angle. C) Scar fill at Tête de Ruch (upper). The higher-density flows either onlap the scar drape abruptly or transform to low-density turbidites up the counter-slope. D) Laterally continuous hybrid beds at Le Marc. These beds are interpreted to have been deposited away from the basin margin and cohesively transformed through distal run-out. 7 cm camera lens (black circle) for scale.

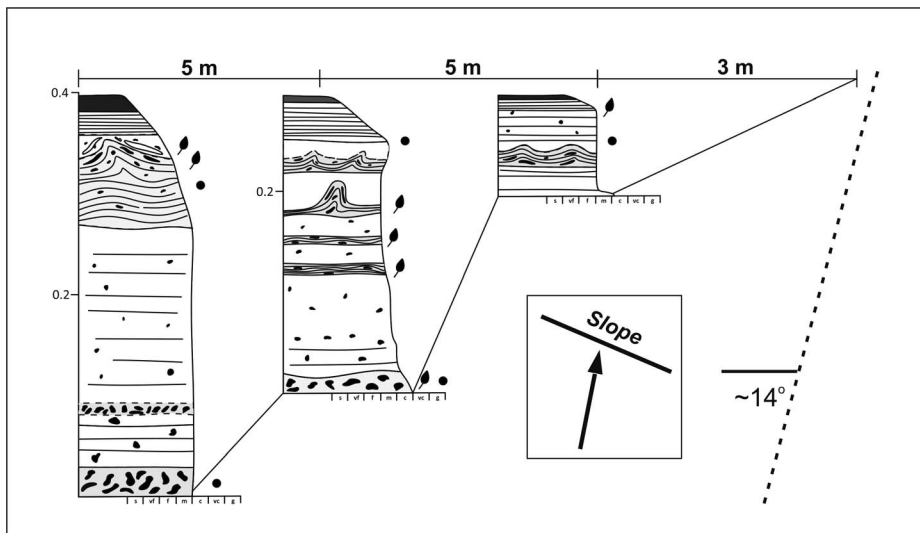


FIG. 12.—High-resolution log of one medium-density turbidite approaching onlap at Col du Fa showing the short length-scale variability seen in these beds.

stratigraphy of the basin, LF 2 commonly has highly irregular bed tops with abundant tractional structures, such as climbing ripples and convolute lamination (Figs. 10E, 12). These beds are termed LF 2B.

Interpretations.—The presence of flutes, normal grading, and tractional structures indicate that the LF 2 beds were deposited by waning, turbulent flows which were able to rework the aggrading deposit (Bouma 1962). This suggests that these flows were more dilute than the parent flows of the thick-bedded sandstones (LF 1). These medium-bedded sandstones are therefore interpreted as medium-density turbidites and are differentiated from low-density turbidites by bed thicknesses being greater than 10 cm and a coarser grain size. These medium-density turbidites also have a thicker massive interval at their base compared to low-density turbidites. Opposing paleocurrent directions within event beds is characteristic of flows encountering topography (e.g., Kneller et al. 1991), indicating that many of these beds were deposited close to a basin margin. Coarser, denser parts of the flow may be more strongly influenced by topography than the upper more dilute part of the same flow (Bakke et al. 2013).

The finer, better sorted and thinner-bedded nature of this lithofacies compared to thick-bedded sandstones indicates that these beds were deposited beyond the axis of the lobe (off-axis) (Prélat et al. 2009; Bell et al. 2018a) (Fig. 8). LF 2B is interpreted as representing flows that were deposited close to the basin margin or possibly within slump scars on the basin margin. Bypassing flows deflected by the margin or trapped in scars caused complicated oscillatory-flow patterns to develop which deformed the aggrading deposits (Pickering and Hiscott 1985; Tinterri et al. 2016; Cunha et al. 2017). An example of this can be seen at Tête de Ruch, where this facies dominates an ~ 10-m-thick scar fill (Puigdefàbregas et al. 2004) and is overlain by thin beds showing simple uniformly directed ripples and plane-parallel lamination (Figs. 5, 11C). These thin beds were deposited over the scar fill where flows were relatively unconfined, allowing more uniform and waning flow deposition to dominate.

FA 3: Proximal Fringe

Observations.—Facies association 3 is dominated by medium- to thick-bedded (0.1–1.2 m) bipartite or tripartite event beds (LF 3) (Figs. 9, 11C, D, G). These beds are composed of a lower division of medium- to thick-bedded sandstone (LF 1 and LF 2) with an irregular top which is loaded and/or eroded into by an overlying argillaceous sandstone (Fig. 10D). The middle division is an argillaceous sandstone, poorly sorted and often deformed, which appears as a sheared fabric (Fig. 10D). The argillaceous sandstone can either contain clasts of the underlying sandstone or be clast-poor. Organic matter (< 70 cm in length) may be present in this bed, with organic-rich sandstones typically thicker than the more argillaceous sandstones. Elongate organic matter is usually aligned with its long axis approximately parallel to paleoflow recorded on the bed base (Fig. 10C).

Argillaceous sandstones, which are rich in cleaner sandstone clasts, commonly occur where the lower, cleaner sandstone is coarser-grained; thus most sandstone clasts seen tend to be coarser grained than the argillaceous matrix. This deposit can show variable sand-to-mud ratios. Higher sand contents within this middle division are associated with increased prevalence of lamination, with centimeter-scale layering (mud-concentrated laminae) sometimes evident, and higher mud contents associated with more sheared and poorly sorted deposits. Both of these divisions may contain coarse-sand to granule-size quartz grains supported within the matrix.

Overlying this argillaceous sandstone, medium-bedded, often muddy sandstone may occur, although it is sometimes difficult to assess whether this sandstone is part of the underlying event bed or represents a separate event bed (Fig. 10D). This sandstone has an irregular base and can show loading and foundering into the underlying argillaceous sandstone (Fig.

10D). The bed top is typically flat or mounded. Approaching basin margins these beds can be seen to transition laterally from thick-bedded sandstones (Fig. 13A, B).

The middle division of the bed may pinch out between the underlying and overlying sandstones, which then amalgamate at the onlap surface (Fig. 13C), forming a complicated and often muddy pinch-out (Fig. 14). Stratigraphically this lithofacies dominantly occurs following the thin-bed-dominated sequence and underlying the medium- to thick-bedded sandstones (Fig. 9).

Interpretations.—The basal and upper sandstones within these bipartite or tripartite event beds are interpreted as either high-density or medium-density turbidites. The massive, poorly sorted, and mud-rich nature of the division encased by these turbidites is interpreted as being caused by en-masse deposition of a laminar and cohesive flow (e.g., Middleton and Hampton 1973; Mulder and Alexander 2001). This bed division is therefore interpreted as a debrite. The irregular contact seen between these divisions has been attributed to complex short-wavelength soft-sediment deformation and erosion (e.g., Fonnesu et al. 2015). Where the overlying turbidite is relatively thick it is difficult to differentiate between a debritic or deformed (see LF 1 basal deformation) origin for the middle division, particularly when the overlying turbidite has foundered into the underlying division (e.g., Fonnesu et al. 2015). Where the middle sandstone division is slightly cleaner, with lamination and/or layering, the sandstone is interpreted as having been deposited by flows transitional between laminar and turbulent and therefore termed a transitional-flow deposit (Baas et al. 2011; Kane and Pontén 2012). These tripartite event beds therefore contain deposits of both turbulent and laminar flow regimes and are subsequently interpreted as hybrid beds (*sensu* Haughton et al. 2003, 2009).

It is suggested that the more organic-rich linked debrites, with decimeter clasts of terrestrial debris, are derived from flows which originated from events in the hinterland that carried significant amounts of terrestrial debris into the marine environment (see also Hodgson 2009). These beds are therefore deposits from particularly high-magnitude flows; this may explain their greater average thickness compared with the more argillaceous hybrid-beds. It is also possible that the organic material was staged for significant periods of time on the shelf, making terrestrial debris a poor indicator of flow magnitude. The close association of terrestrial debris and coarse grain sizes in these relatively distal environments, however, indicates that these beds were the result of high-magnitude or “outsize” flows that were capable of significant substrate erosion (Fonnesu et al. 2018). Incorporation and disaggregation of this eroded substrate will have primed these flows for rheological transformation (Kane et al. 2017; Fonnesu et al. 2018). LF 1 can be seen to transform into these hybrid beds over tens of meters approaching the slope, further indicating that these beds were highly erosive and prone to rheological transformation, even in proximal positions, due to forced deceleration against the basin margin (e.g., Patacci et al. 2014). The presence of large amounts of erodible and muddy draping substrate on the basin margin will aid in short-length-scale flow transformation in these high-magnitude flows (Fig. 14) (e.g., Fonnesu et al. 2018).

It is possible that the debritic division of these beds represents high-concentration turbidity currents hitting the counter-slope, causing intra-basinal slope instability and failure. The turbidity current will then have aggraded around this failure, represented positionally by a sandwiched debrite (e.g., McCaffrey and Kneller 2001). It is difficult to differentiate between a flow-transformation or slope-failure origin for the co-genetic debrite at outcrop; however, the presence of large organic clasts within an identified debritic division may favor a flow-transformation origin.

Because these beds dominantly underlie the thicker-bedded and more sandy turbidites of FA 1 and 2, they are interpreted as being positionally adjacent (*sensu* Walther 1894) (Figs. 8, 9). An abundance of hybrid beds indicates a more distal lobe sub-environment compared with the axis and off-axis deposits of FA 1 and FA 2 (e.g., Hodgson 2009; Jackson et al.

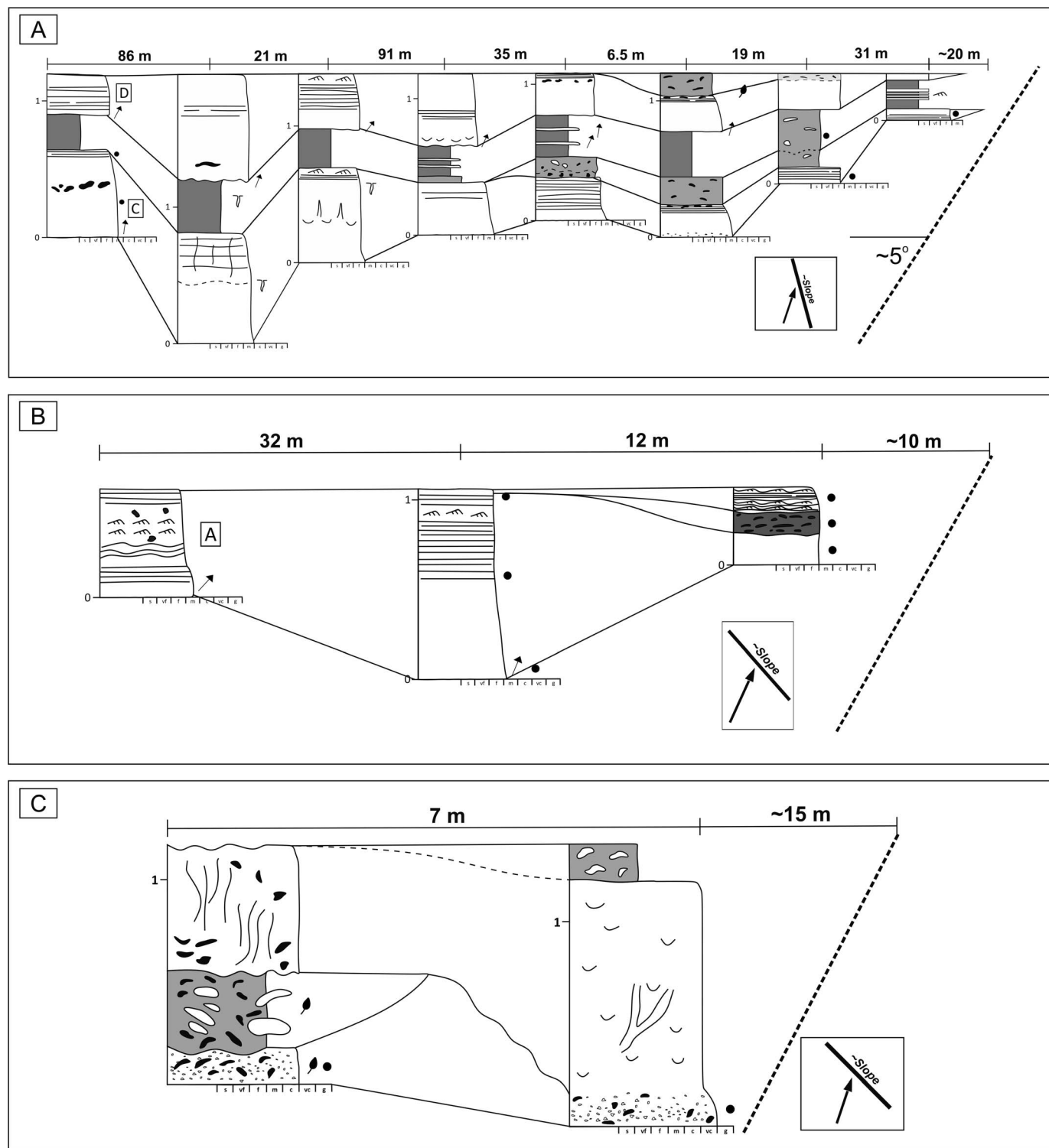


FIG. 13.—**A**) Hybrid-bed evolution approaching topography at Argenton. **B**) Hybrid evolution at Tête de Ruch (lower). **C**) Hybrid-bed evolution at the Tête de Ruch (upper). The complex interaction between the debritic and turbiditic intervals are suggested to result from either differential interaction with the slope between rheologically distinct flow phases or erosion at the onlap surface. Letters in blacked boxes = correlated bed label. Log key in Figure 5.

2009; Kane et al. 2017; Fonnesu et al. 2018). This sub-environment is termed the lobe fringe. FA 3 is therefore interpreted as being analogous to lobe-fringe deposition seen in unconfined systems (e.g., Spychala et al. 2017). The lobe fringe can be further subdivided into a lateral and frontal

fringe, with the lateral fringe having a lower proportion of hybrid beds compared to the frontal fringe (Spychala et al. 2017). In confined settings this definition is complicated because flow deceleration against lateral slopes causes flow transformations and subsequent enrichment of hybrid

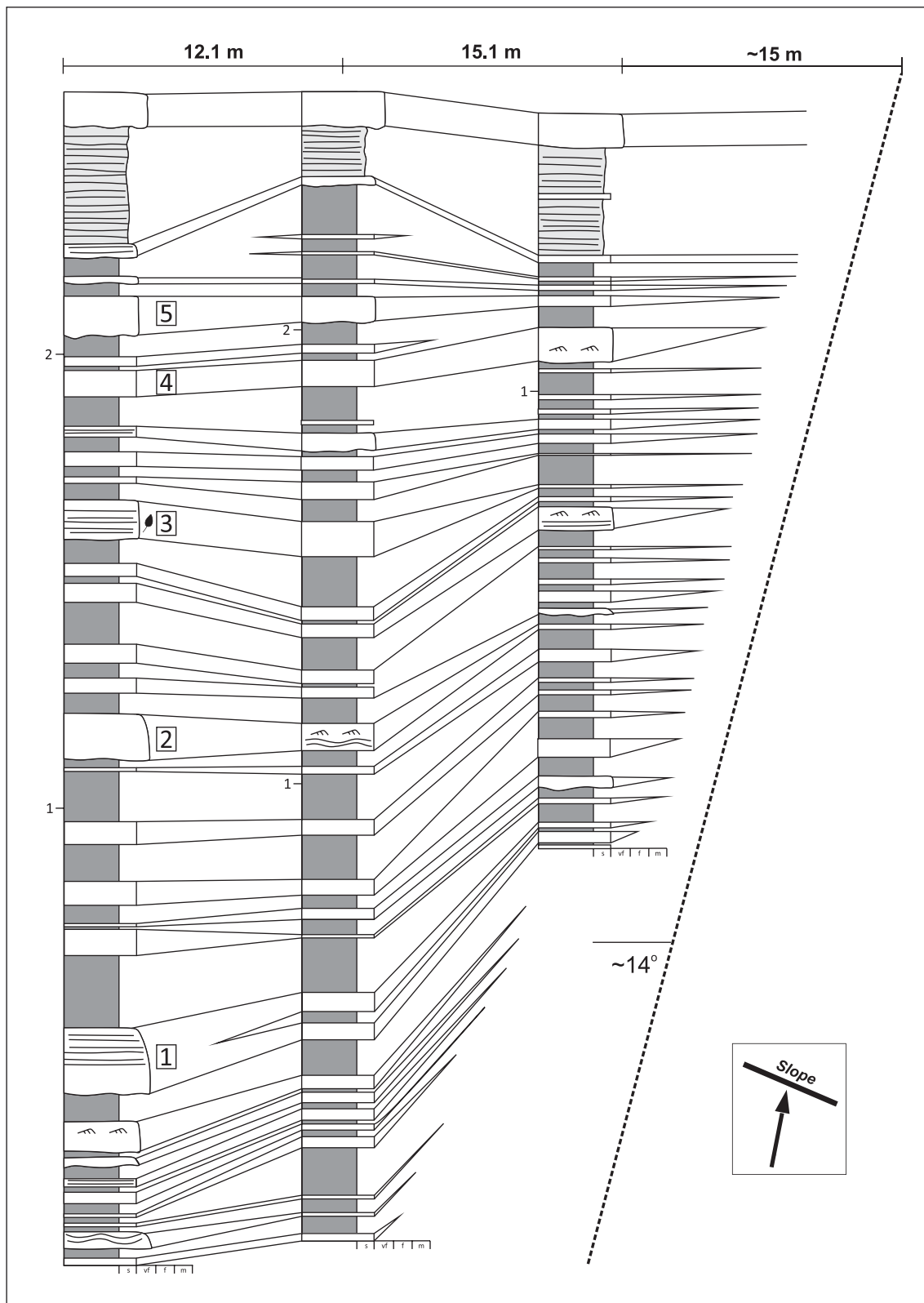


FIG. 14.—Example of correlated low-density turbidites approaching the Col du Fa basin margin. Very little facies variation is seen in these beds.

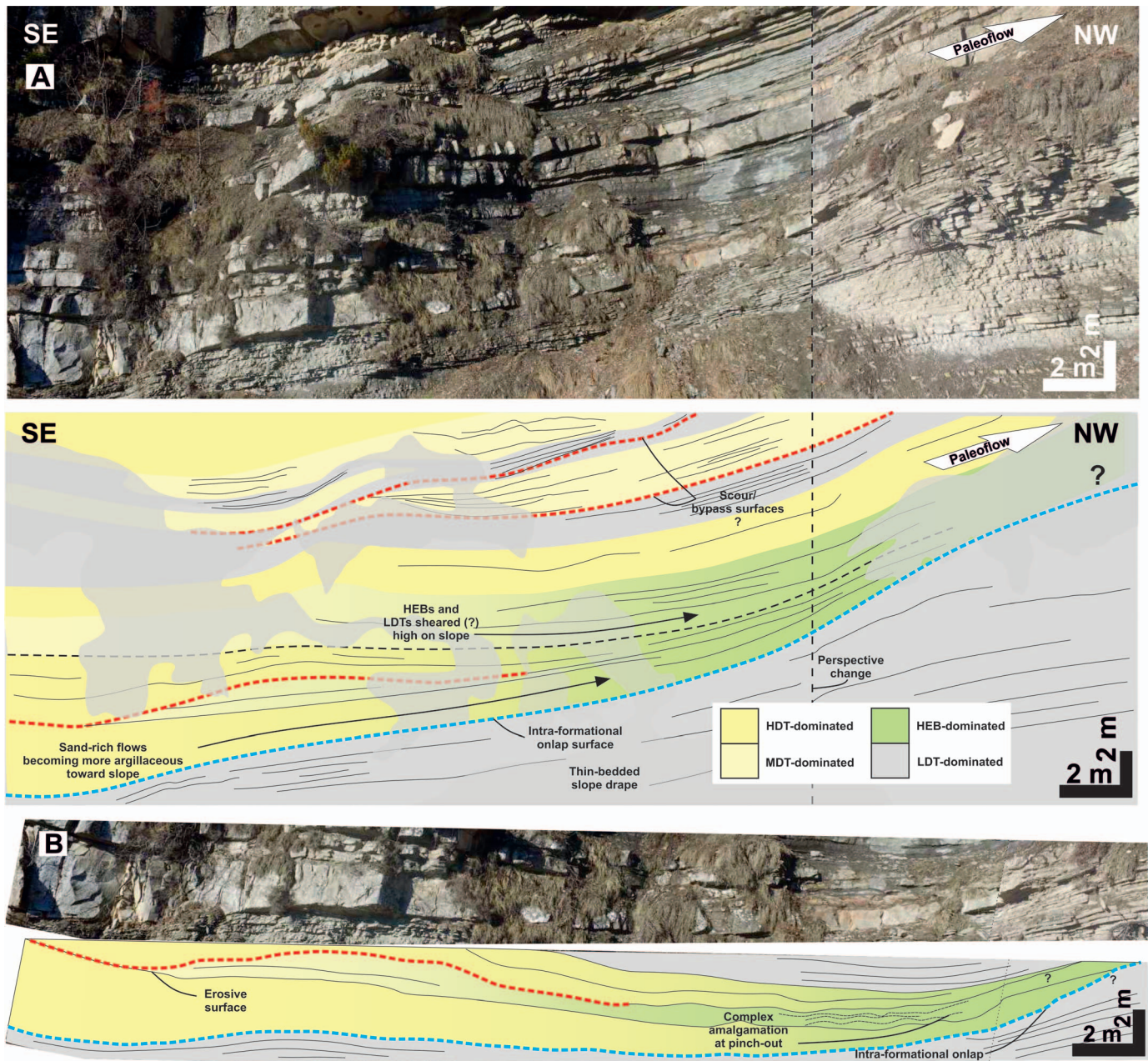


FIG. 15.—Outcrop sketch from the Col du Fa locality. **A**) Low-density turbidites drape the slope and are onlapped by hybrid beds and higher-density turbidites. **B**) Flow transformation can be seen to occur in the proximal fringe deposits over 10–15 m approaching the onlap surface to the NW, resulting in complex amalgamation zones at pinch-out (see Fig. 10D for pinch-out detail).

beds in the lateral fringe (Figs. 8, 14, 16, 17). This relationship is also evident in the Late Cretaceous Britannia Sandstones of the North Sea, where flows underwent rheological transformation against a lateral slope (Lowe and Guy 2000; Barker et al. 2008). This study thus uses the general term proximal fringe because the frontal and lateral fringe are expected to be similar due to the counter-slope causing a prevalence of hybrid beds in both settings (Figs. 8, 14, 17).

It should also be noted that particularly erosive flows in the lobe axis and off-axis also generate hybrid beds at the onlap surface (e.g., Patacci et al. 2014; Fonnesu et al. 2018). This can make lobe-sub-environment interpretation challenging when adjacent to a steep basin margin because much of the succession may be margin-affected over short length scales

(tens of meters) (Fig. 14) and therefore not represent their primary lobe-scale paleogeographic position (e.g., Southern et al. 2015). This is enhanced in tectonically active basins where flow types can be highly variable (e.g., Mutti et al. 2009). Facies back-stripping may therefore need to be attempted to assess the lobe-scale sub-environment (Fig. 16). These short-length-scale margin effects and attempts at back-stripping are summarized in Figures 16 and 17.

FA 4: Distal Fringe

Observations.—Facies association 4 is dominated by thin-bedded (0.01–0.1 m) siltstones to fine-grained sandstones (LF 4) that form laterally

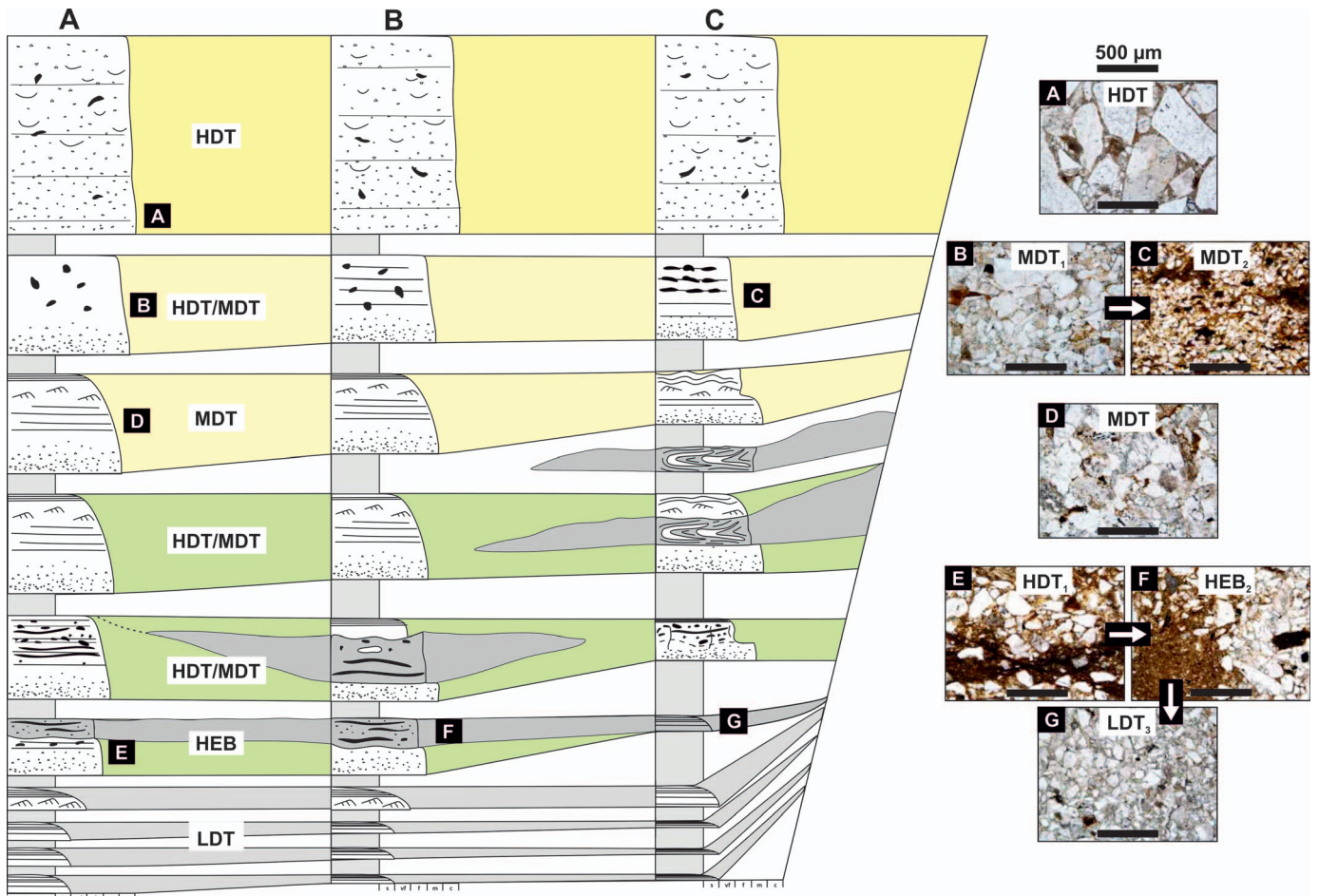


FIG. 16.—Summary logs showing facies transition approaching pinch-out toward basin margins for given lobe sub-environments and their dominant facies. The right-hand petrographic images are taken from representative beds in the Annot Basin approaching onlap. The corresponding letter (white text in black box) on the logs indicates the point in the bed where the sample was taken. Onlap to right.

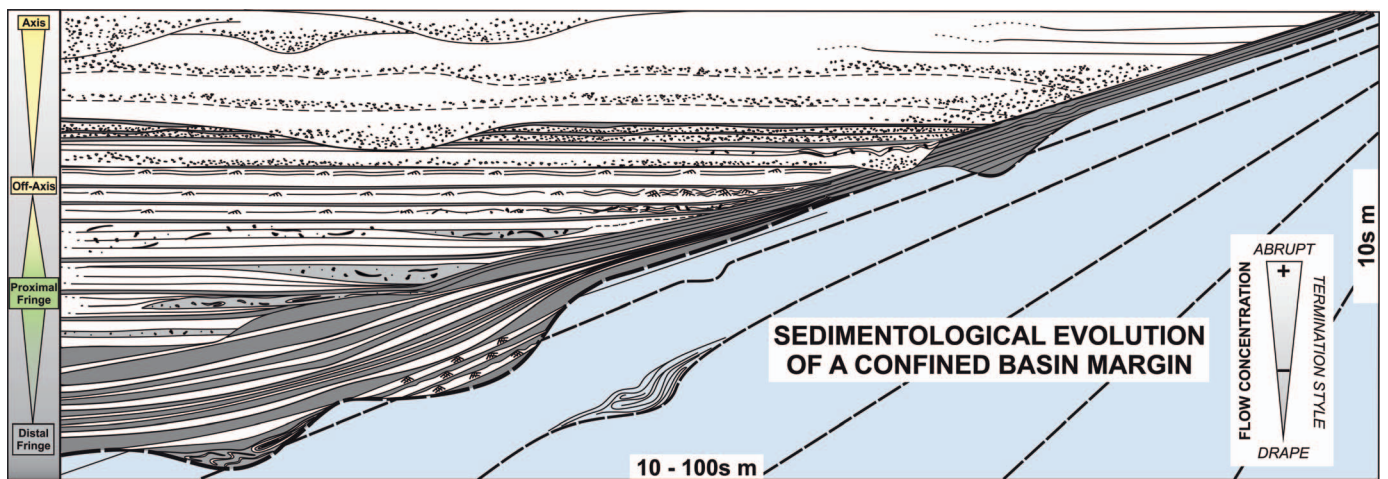


FIG. 17.—Synthesis of facies evolutions seen in the Grès d'Annot towards the basin margins and their stratigraphic position. Flow concentration at the point of sedimentation largely controls the style of the onlap termination. Lobe sub-environments are often obscured adjacent to onlap surfaces due to topographic interaction between the flow and the slope, but can be back-stripped.

continuous event beds (Figs. 7, 11A, 13). Parallel and convolute lamination is common (Fig. 10F). Beds are normally graded, with ripples common on bed tops (Fig. 10F). Ripples may show multiple and opposing paleocurrent directions within single beds. Beds tend to pinch out over tens to hundreds of meters towards the basin margin (Fig. 15), with amalgamation of event beds sometimes observed towards the onlap surface, causing local bed thickness increases in a regional thinning trend. Slumping and folding of beds (LF 5) is evident in this FA, particularly immediately underlying the abrupt transition to dominantly medium- and thick-bedded sandstone sequences (Fig. 10G). Fold-axis measurements indicate that deformation was both oblique and perpendicular to paleo-slopes. Stratigraphically, these beds immediately overlie the Marnes Bleues, forming a distinct sequence that significantly drapes the Marnes Bleues slope (11A). This lithofacies becomes less common up stratigraphy (Fig. 9).

Interpretations.—The fine grain-size, abundance of tractional structures, and dominance of thin beds within LF 4 indicates deposition from dilute, low-density turbidity currents (*sensu* Lowe 1982). The narrow grain-size range (dominantly silt) of these slope-draping beds is numerically predicted because of the quadratic decrease in settling velocity of silt and mud and the consequent increase in likelihood of flow inflation far above the initial flow depth in silt- and mud-rich flows (Dorrell et al. 2019). Because these beds are able to drape the existing relief they are suggested to have healed much of the initial relief present on the Marnes Bleues slopes (Figs. 7, 11A). Slumping in these successions (LF 5) is interpreted to represent slope failure on the steep basin margins (Fig. 10G). Progressive deformation and seismicity along the Alpine thrust front is suggested as the primary reason for slope failure (Fig. 2). Failure scars may contribute to some of the heterogeneity seen within the overlying medium- and thick-bedded sandstones by creating a rugose topography high on the slope (Fig. 11C).

The lateral continuity, fine grain-size and thin-bedded character of the thin beds is consistent with both levee deposition and lobe-fringe deposition. Because of the few long-lived channels identified and the low stratigraphic position of these beds in a prograding lobe (Fig. 9), they are not interpreted to be levee deposits, but are instead attributed to the distal fringe of a submarine lobe on the basin floor (e.g., Boulesteix et al. in press, Boulesteix et al. 2019) (Fig. 8), which caused termination of Marnes Bleues carbonate deposition. This is supported by the published paleogeographic position of the lowermost Grès d'Annot (Fig. 2) (Apps et al. 2004; Joseph and Lomas 2004; Salles et al. 2014). The relative lack of hybrid beds in the LF 5 sequence also supports a distal lobe fringe interpretation (Figs. 8, 9A, 13) (Spychala et al. 2017).

STACKING PATTERNS

Le Ray

Confined basins have previously been associated with sheet-like deposition, where incoming flows are entirely confined by the basin margins, resulting in tabular stratigraphy with little or no autogenic compensational stacking (e.g., Sinclair and Tomasso 2002). Numerical studies (Dorrell et al. 2018), subsurface studies (e.g., Beaubouef and Friedmann 2000), and outcrop studies (e.g., Spychala et al. 2016; Bell et al. 2018b; Liu et al. 2018), however, have shown the stacking-pattern complexity that may arise in basins that display variable degrees of confinement. This study uses data from the lowermost member of the Grès d'Annot, the Le Ray member (Figs. 5, 6), to build on these studies. Le Ray (Puigdefàbregas et al. 2004), or member A (Du Fornel et al. 2004), was fully confined by the basin margins during its deposition (Callec 2004; Salles et al. 2014).

Unit 1.—This unit comprises a sequence of thin-bedded low-density turbidites (LF 4) overlain abruptly by medium- and thick-bedded high-

density turbidites (LF 1 and 2). These thick-bedded sandstones correlate with a thick sequence of thin-bedded turbidites ~ 800 m to the NW adjacent to the Braux Fault footwall (Figs 3, 6). This transition is caused either by flow over-spill across the paleobathymetry of the Braux Fault or draping of the lower-density part of the flow up the Braux Fault topography. Correlation of this unit toward the NE is hindered by lack of exposure; however, it is possible that the distal Unit 1 correlates with some of the early Unit 2B deposition (Fig. 6).

Unit 2.—Proximal Unit 2 is characterized by a thick 33 m amalgamated sandstone body interpreted as being deposited by high-concentration turbidity currents. Indicators of erosion, such as scours and decimeter-scale mud-clasts, indicate that this was a region of significant bypass (e.g., Stevenson et al. 2015) and is interpreted to represent the lobe axis (FA 1) through Le Ray deposition. Down-dip this unit has been subdivided into Unit 2A and 2B based on facies and stacking. Unit 2B is composed of thin-bedded turbidites that drape the frontal confinement of the early Annot Basin and stack aggradationally (Fig. 11A). This confinement was caused by a combination of the basin closure due to the NW–SE Melina anticline, the E–W Fuguret anticline, and the NE–SW Braux Fault (Fig. 3). Unit 2A represents an abrupt transition into thicker-bedded sandstones that pinch out against the underlying Unit 2B. These sandstones can be subdivided into various lobes based on the correlation of intervening packages comprising low-density turbidites (LF 4) overlain by hybrid beds (LF 3), medium-density turbidites (LF 2), and amalgamated high-density turbidites (LF 1), which are interpreted to represent the sequential stacking of distal-fringe (FA 4), proximal-fringe (FA 3), off-axis (FA 2), and axis deposits (FA 1). These lobes represent the depositional products of the bypassing flows from the proximal thick sandstone body, forming the lobe axis.

The axis of each of these lobes steps farther into the basin, suggesting allogenic progradation through increasing sediment flux from the uplifting Corsica–Sardinia hinterland (e.g., Apps et al. 1987). This pattern is not uniform, however, and a degree of compensational stacking is clearly visible, with the axes of successive lobes (represented by amalgamated high-density turbidites) overlying the fringes of underlying lobes, which represented lows on the seafloor (e.g. Deptuck et al. 2008; Prélat et al. 2009). These stacked lobes could also represent lobe “fingers” that were focused between the lows of the previous axial deposits (e.g., Groenenberg et al. 2010). In this case the apparent basinward stepping of the Le Ray lobes may be autogenically-driven, as flows are focused between the lows and build passively into the basin. This explanation may operate in tandem with allogenic progradation, particularly during early deposition, due to the prevalence of these finger-like geometries in the basal stratigraphy of lobe complexes (e.g., Prélat et al. 2009; Groenenberg et al. 2010). These indicators of compensational stacking are at odds with the prevailing suggestion that basins generically described as “confined” can be assumed to have a sheet-like architecture, and fit with the recent work indicating that lobes deposited within basins with varying degrees of confinement are characterized by more complicated stratigraphic relationships (e.g., Marini et al. 2015; Bell et al. 2018b; Liu et al. 2018).

The presence of thick and coarse sandstones in distal positions has also been described in subsurface datasets of submarine lobes and lobe elements and has been attributed to flow stripping of the upper dilute parts of flows over the basin's confining topography, leaving behind the coarser parts of the flow (e.g., Marini et al. 2016; Jobe et al. 2017). This process may also contribute to the preservation of the thick and abruptly terminating sandstones within Unit 2A of the Le Ray member.

Unit 3.—This unit has been differentiated because it cannot be reliably correlated to another unit. It is possible that Unit 3 represents the distal expression of the upper parts of Unit 2, however the lack of exposure between the proximal and distal parts of the upper Le Ray prevents reliable correlation.

Alternative Interpretations.—The observed intra-formational onlap against the low-density fringe (Unit 2B) at the Col du Fa locality is likely caused by the inferred proximity of the basin margin. An alternative explanation for this stratigraphic relationship may be the presence of a large erosional feature, such as a scour, at the Col du Fa margin. Such scours are interpreted higher in the basin stratigraphy at Tête du Ruch (e.g., Puigdefàbregas et al. 2004), and show the same intra-formational onlap relationship (Fig. 11C). Decameter-thick scour fills are also suggested to be present in the Grès d'Annot at Peira Cava (Lee et al. 2004). The scour would have created accommodation space to be filled by the incoming flows, resulting in the onlap geometries described by this study. Exposure limits further analysis of this problem, however, a scour interpretation is not believed to affect the underlying principles of this study as the low-density turbidites still drape the scour and are onlapped by the later higher-density turbidites.

Another explanation for the observed intra-formational onlap may be that the low-density fringe (Unit 2B) was tilted (e.g., Salles et al. 2014) and subsequently onlapped by higher-density flows when the basin was relatively static or depositional rates were higher, resulting in the wedge-shaped geometry observed (Apps et al. 2004). Unit 2B may therefore represent the distal extents of early Le Ray (i.e., Unit 1), while the onlapping Unit 2A is either more proximal and late-stage Le Ray or early La Barre (i.e., Unit 3) (Figs. 3, 5). Differential compaction between the basin center and the basin margin may have also acted to enhance the tilting effect (Sinclair 1994). The inability to walk out individual units between outcrop localities again makes further analysis of this problem difficult. If tectonism or differential compaction is the reason for the observed relationship, then run-up of the low-density turbidites that characterize Unit 2B would have acted to exaggerate the intra-formational onlap that was caused by tilting, and the underlying principles of this study are maintained. Unit 1 would therefore be analogous to the ponded aprons identified in intra-slope basins of the Gulf of Mexico, while Unit 2 would be similar to a perched apron (Prather et al. 2017).

Turbidity-Current Run-Up and Onlap Geometry

Sediment gravity flows are able to deposit high on confining slopes through flow run-up and/or inflation (e.g., Muck and Underwood 1990; Lamb et al. 2008; Dorrell et al. 2019). The distance a turbidity current runs up topography is termed the run-up height (H) and, in its simplest form (following Straub et al. 2008), can be represented by,

$$H = h + \frac{\rho_c U^2}{(\rho_c - \rho_a)2g} \quad (1)$$

where h = flow thickness, U = flow velocity, ρ_c = bulk density of the flow (composed of quartz at 2650 kg m^{-3}), ρ_a = density of the ambient water (seawater at 1020 kg m^{-3}), and g = acceleration due to gravity (9.81 m s^{-2}). In order to assign a single value for sediment concentration there is an assumption that there is no density stratification within the flow. A 30-m-deep channel-form at Chambre du Roi (Sinclair 2000) has been used as the basis for estimating minimum flow height. This is slightly arbitrary but serves the purpose of this thought-experiment. In order to correct for channel-related superelevation, this flow height has been multiplied by 1.3 (see Mohrig and Buttles 2007), giving a h value of 39 m. This height represents the minimum height of the flow at the lobe apex, disregards compaction, and is assumed constant. It should be noted that due to a lack of flow-height proxies preserved at outcrop, this value is used purely to demonstrate the underlying principles of the model, i.e., the model does not attempt to fully reconstruct the turbidity currents entering the Annot Basin. The depth-averaged flow velocities used range from 5 m s^{-1} to 0.5 m s^{-1} . The upper limit of 5 m s^{-1} is derived from the maximum flow velocities ($4\text{--}6 \text{ m s}^{-1}$) reached by sand-rich flows in the Monterey Canyon (Symons et al. 2017), while the lower limit of 0.5 m s^{-1} is derived from

average measurements of finer-grained flows in the Congo Canyon (Azpiroz-Zabala et al. 2017). The Annot system is sand-rich; therefore the faster Monterey flows are likely the most analogous, at least close to the input. Flow velocity will decrease with decreasing concentration, making the use of a constant velocity problematic. This is suggested to be less important for small and confined basins, such as the Annot Basin, where flows may be prevented from significant velocity decay between the axis and pinch-out. If velocities do decay significantly, then plotting single velocity values through the height of an individual flow will be required; for example, the 5 m s^{-1} and 10% concentration basal part of a hypothetical flow will run-up 9.2 m above the flow height, while its 1 m s^{-1} and 0.1% concentration tail will run-up 32 m above the flow height. This decameter scale difference may explain the $\sim 15 \text{ m}$ of slope drape at Col du Fa (Figs. 6, 8). This parameter is further complicated by the possible presence of low-velocity dense basal layers within highly-concentrated stratified flows (e.g., Stevenson et al. 2018). Turbulence is suppressed in these basal layers; this reduces velocity and run-up heights, resulting in the increased likelihood of an abrupt pinch-out of the sand-rich basal layer and bypass of the upper and low-concentration parts of the flow. The wedged high-density turbidites identified at onlap by this study (Fig. 11B) may be the depositional products of such basal layers.

By varying flow concentration in equation (1), a clear trend is developed, with lower sediment concentrations resulting in greater run-up heights (Fig. 18A). In prograding lobe systems turbidity currents with lower sediment concentrations (well below 10%), forming low- or medium-density turbidites, are typically found in the distal or basal stratigraphy and flows with higher sediment concentrations ($> 10\%$), forming high-density turbidites, are typically found in the proximal or upper stratigraphy (e.g., Hodgson et al. 2006, 2009; this study). This therefore suggests that earliest turbulent flows into a receiving basin should have the greatest run-up heights, assuming all of these flows are of similar thickness, with run-up heights decreasing through time as flows become more concentrated (Fig. 18A). It should be noted that the effect of increasing concentration through time will be counteracted by increasing velocities, as discussed previously. Suspended-sediment concentrations of $> \sim 8\%$ have been shown to suppress the generation of current ripples and cause transformation from turbulent to transitional flow, where flows decelerate sufficiently, forming transitional or hybrid-flow deposits (Baas et al. 2011). This concentration ($> \sim 8\%$) has therefore informed the placement of hybrid beds along the x axis of the run-up height trend (Fig. 18A), giving hybrid beds a similar run-up potential as high-density turbidites. It should be noted that Baas et al. (2011) emphasize that this value is dependent on flow velocity, grain size, and sediment composition, and that the dimensionless Reynolds number is a much better predictor of flow phase. The results of this analysis fit with facies-dependant thinning rates compiled from 18 outcrop studies by Tórkés and Patacci (2018), with hybrid-beds having 1.3 to 2.8 times higher thinning rates than turbidites. Data collected in this study also support the compiled data of Tórkés and Patacci (2018), with thinner-bedded turbidites having lower thinning rates than thicker-bedded turbidites and consequently draping topography (Figs. 6, 7, 14). Similar thinning trends have been reported from levee sandstones (DeVries and Lindholm 1994).

Lateral vs. Frontal Onlap

To assess the run-up variation between frontal and lateral onlap the velocity of the modeled flow (at 5% concentration) was varied according to the incidence angle of the flow with the slope. It is assumed that the flow velocity will be at its maximum (5 m s^{-1} in this case) in the principal direction of travel, or an angle of incidence of 90° with respect to the slope, and that the flow velocity will fall to 0 m s^{-1} perpendicular to its axis at an angle of incidence of 0° , i.e., when the flow is running perpendicular to the topography. In reality there will still be some lateral velocity; however, for

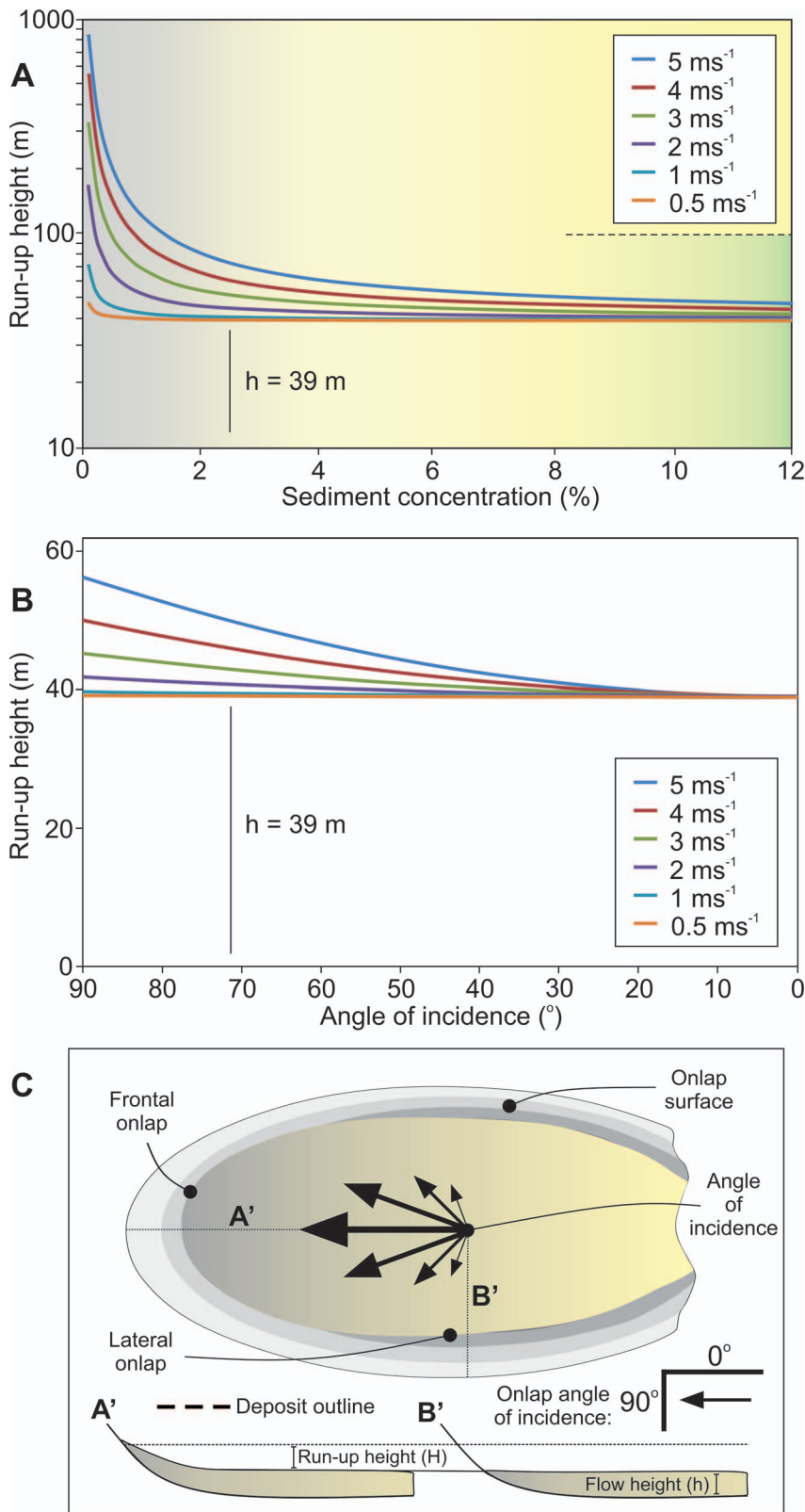


FIG. 18.—**A**) Run-up height versus flow sediment concentration for flows of varying velocities. Flows with high concentrations are less able to run up topography than low-concentration flows if all other parameters are equal. **B**) Run-up height versus the angle of incidence between the flow and the slope for flows of varying velocities. Lower angles of incidence cause higher run-up of flows. **C**) Schematic diagram showing the relationship between frontal and lateral onlap (modified from Al A'Jaidi et al. 2004).

the purposes of this simple analysis it is assumed that this is negligible. The fastest flows occur at an angle of incidence of 0° or perpendicular to the slope (Fig. 18B). These flows therefore run farther up the counter-slope. Deposits of these flows would pinch out higher up the frontal slope than

the lateral slope (Fig. 18B, C). In the 5 ms⁻¹ case, for example, the difference in run-up height between the frontal and lateral part of the flow is 17 m. The difference will be increased in lower-density flows and reduced in slower flows.

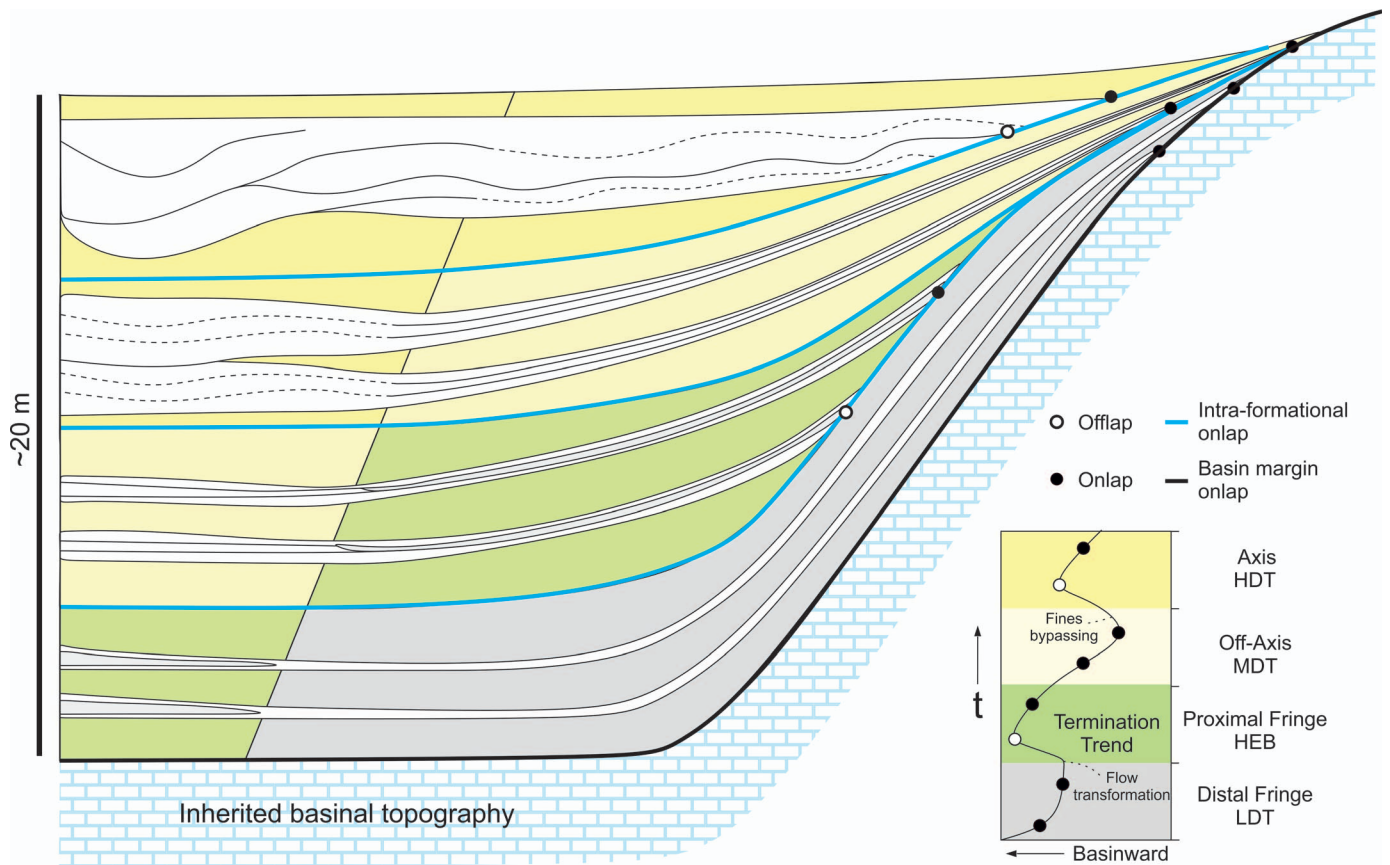


Fig. 19.—Model for the stratigraphic evolution of flow terminations in a static confined deep-water basin. It is suggested that the pattern of termination trends may be used to predict the termination style expected at a given point on the onlap surface. Flow transformation results in highly concentrated flows, which may result in offlap. Similarly, bypass of the upper parts of axial flows results in offlap of the deposits of the highly concentrated basal layers of these flows against the underlying deposits. Concurrent hemipelagic deposition has been ignored for simplicity.

DISCUSSION

Stratigraphic Evolution of Onlap

Based on the similarity between facies transitions and associations seen in this confined basin and those in unconfined or weakly confined submarine lobes (Figs. 8, 9) (e.g., Hodgson 2009; Spychala et al. 2016, 2017), and the onlap termination styles shown by this study to be produced by the parent flows of these facies (Figs. 16, 17), a predictable stratigraphic evolution of onlap at confined basin margins is proposed (Fig. 19).

Distal Fringe.—Initially, onlap terminations will be characterized by draping of the slope as low-density turbidites of the lobe fringe are deposited (Figs. 17, 19). This low-density turbidite drape is likely to be composed predominantly of silt or mud, because fine-grained flows are much more capable of flow inflation and deposition high on the slope (Dorrell et al. 2018). It is also suggested that much of the poorly-exposed hemipelagic sediment in deep-marine basins is composed of millimeter-scale and centimeter-scale event beds (Fig. 10F) (Boulestex et al. in press, Boulestex et al. 2019), and consequently represents the distal lobe fringe. Lobe-fringe deposition is therefore likely to be more widespread than previously appreciated (Boulestex et al. 2019b; Spychala et al. 2019) and results in the healing of substantial amounts of basinal topography, forming a dominantly aggradational sequence of thin beds on the basin margin (Figs. 11A, 17, 19).

Proximal Fringe.—Hybrid beds and low-density turbidites of the proximal lobe fringe are then deposited into the basin as the system

progrades (Fig. 19). These hybrid flows are more concentrated and will therefore have lower flow efficiencies when they encounter the slope, so will be unable to deposit as far up the slope as the underlying low-density turbidites of the distal lobe fringe (Figs. 17, 18A). This will cause abrupt intra-formational onlap of these higher-concentration flows against the underlying lobe-fringe deposits (Fig. 19). In the Annot Basin this is represented by proximal-fringe deposits wedging out against the underlying distal-fringe deposits (Figs. 11A, 14). The abruptness and complex 3D geometry of these terminations is enhanced by the combined potential for hybrid-bed development through long-run-out cohesive flow transformation (e.g., Haughton et al. 2009), slope-induced flow transformation (e.g., Barker et al. 2008; Patacci et al. 2014; Bell et al. 2018b), and flow-induced slope failures (e.g., McCaffrey and Kneller 2001) (Fig. 16). This depositional pattern will be seen in cross sections as a progressive migration of termination points towards the basin center (offlap) (Fig. 19) or a reduction in distance between successive onlapping termination points towards the basin margin. Sylvester et al. (2015) generated similar onlap trends using a geometric approach with subsidence and sediment supply as the variables.

Off-Axis.—As progradation continues, these hybrid-bed-prone proximal-fringe deposits will become overlain by deposits of more proximal flows which have not decelerated to the same degree and hence are more turbulent and of lower concentration, but sand-rich (Figs. 17, 19). The off-axis deposits will be able to drape the slope more effectively than the underlying hybrid beds owing to their lower sediment concentrations (Fig.

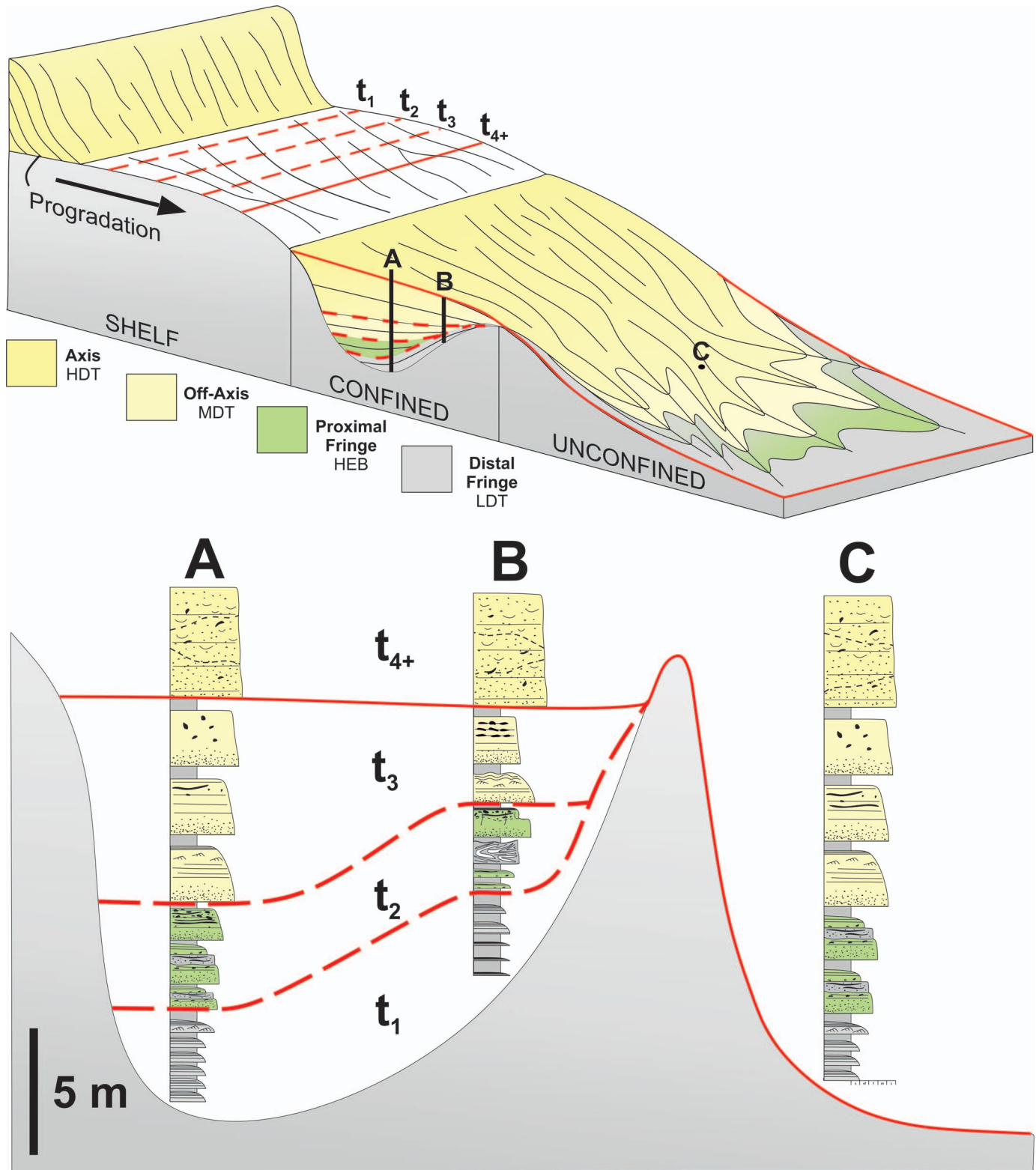


FIG. 20.—Model for the progradation of a clastic system into an intra-slope minibasin. Representative logs (A, B, and C) of the various sub-environments are indicated.

19). This will result in progressive termination of their deposits higher up on the slope and either intra-formational onlap against the now thinner veneer of the low-density fringe or onlap directly against the hemipelagic basin margin (Figs. 17, 19, 20, 21).

Axis.—As higher-concentration flows begin to dominate, intra-formational onlap may occur against the underlying fringe or off-axis deposits that were able to run up the hemipelagic slope (Fig. 19). The highly concentrated basal layers of these flows will be preserved as abruptly

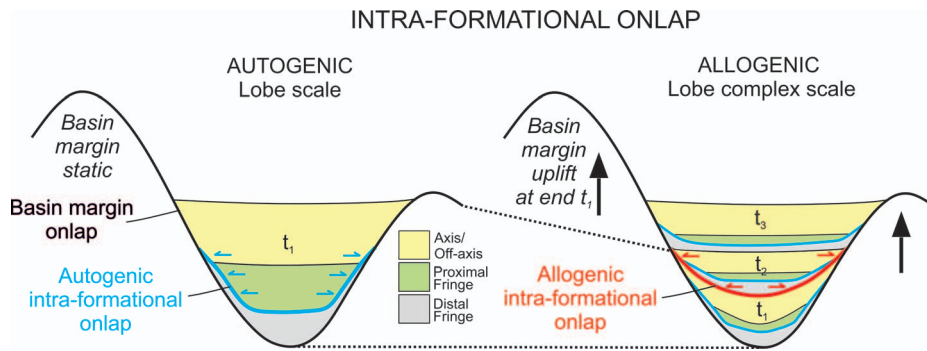


FIG. 21.—Types of intra-formational onlap that can be recognized in confined deep-water basins (modified from Sinclair and Tomasso 2002). A distinction is made between autogenic onlap, caused by longitudinal flow evolution over shorter timescales, and allogenic onlap, caused by tectonic subsidence over longer timescales. Autogenic processes will create short-length-scale heterogeneities in larger-scale and allogenicly controlled sequences.

onlapping high-density turbidites, with the low-density tail of the flow bypassed down-dip. These axial flows will also be more erosive and able to incorporate mud-rich substrate, resulting in an increasing likelihood of intra-formational onlap through short-length-scale rheological flow transformation and consequent higher thinning rates adjacent to the basin margin (Fig. 14). The scours formed by these erosive events close to onlap will promote further autocyclic modulation of stacking patterns adjacent to the basin margin (e.g., Eggenhuisen et al. 2011). This relationship will also be exaggerated in coarser-grained systems because higher concentration flows will be less able to deposit farther up the slope, particularly at lateral margins if these high-concentration flows are narrower (Al-Jaidi et al. 2004).

A critical point in the basin fill will then be reached when these deposits heal the confining topography sufficiently to allow bypass of the coarser components of flows over the confining slope, forming a stepped, instead of a ponded, basin (Prather et al. 2017). Until this level is reached the finer-grained parts of the flows were stripped, thus increasing the sand proportion in the up-dip basin (Prather et al. 2017). This transition is represented toward the sill of the Annot Basin, where proximal lobe-axis deposits bypass down-dip to the Grand Coyer minibasin (Fig. 2), where this stratigraphic evolution repeats in the next confined depocenter.

In the case that the topography is sufficient so as not to be healed by the underlying deposits, the lobe-axis deposits will continue to onlap against the underlying deposits until the accommodation is healed sufficiently to allow the axial deposits to onlap against the hemipelagic basin margin or completely fill the basinal relief and behave as essentially unconfined deposits, resulting in downlapping terminations (Fig. 19). Apparent unconfinement in a vertical section may also occur if allogenic progradation (e.g., increasing sediment flux) does not keep pace with topographic healing. This will result in the axial sandstones rarely onlapping directly against the constantly retreating basin margin and instead depositing away from the slope and on the basin floor (e.g., Kneller and McCaffrey 1999).

Applicability and Limitations

Syn-Depositional Deformation.—This general stratigraphic evolution applies most readily to static basins with little syn-depositional deformation, where onlap trends are not modified by changes in subsidence or depocenter migration (Figs. 19, 21). The Annot Basin was subject to syn-depositional movement of the depocenter (e.g., Salles et al. 2014); however stratigraphic units of the basin fill show the same conceptual evolution as hypothesized for a static basin (Fig. 6), with the only difference being that the onlap is exaggerated on the tilted eastern exposures because of the increasing slope angle during deposition (Fig. 11A) (Salles et al. 2014). In salt-deformed basins, where syn-depositional subsidence can be rapid, this onlap evolution will be also be exaggerated. The general model for onlap evolution (Fig. 19) may therefore broadly apply to actively deforming basins (Fig. 21). It may be difficult, however,

to differentiate between allogenic onlap patterns caused by syn-depositional subsidence or sediment flux (e.g., Sylvester et al. 2015) and those caused by autogenic variations in flow properties (Fig. 21). Care therefore needs to be taken when reconstructing tectonic histories from onlap trends alone, especially in datasets without lithological control.

Onlap Incidence Angle.—Frontal onlap causes greater turbidity current run-up than lateral onlap (Fig. 18B, C). This in turn makes the model presented here more applicable for dip sections against a confining slope. This is further reinforced by the Le Ray dip-oblique correlation (Fig. 6), which is interpreted to record the stratigraphic evolution of onlap described. The lack of a significant thin-bedded slope drape at the lateral onlap of Grès d'Annot at Chalufy (e.g., Puigdefàbregas et al. 2004; Smith and Joseph 2004) may be an example of the importance of incidence angle, with run-up decreased against the lateral slope (Fig. 18B, C).

A minor thin-bedded slope drape does exist at Chalufy, however, and intra-formational onlap does occur against these thin beds (e.g., Bakke et al. 2013). This relationship may occur against lateral margins because flows become increasingly elongate with increasing sediment concentrations (Al-Jaidi et al. 2004). In strike sections this will result in a similar onlap termination pattern, with thicker and lower-concentration flows of the lobe fringe depositing higher on the lateral slope than higher-concentration flows of the lobe axis, which are elongated in the dip direction and more prone to bypass down-dip. This relationship may therefore apply to both strike and dip exposures; however, greater understanding of frontal vs. lateral onlap in exposed or subsurface deep-water systems is required for further analysis.

The lack of a substantial thin-bedded drape at Chalufy may also be caused by its relatively distal position compared to the Annot Basin (Fig. 2), resulting in lower-velocity and lower-concentration flows being unable to maintain enough energy during their longer passage down the slope to deposit significant thicknesses of sediment high on the confining slopes (Fig. 20).

Hierarchical Scale.—The onlap patterns observed in this study are seen mainly on the scale of tens of meters, similar to typical lobe or possibly lobe-complex dimensions (Prélat et al. 2009). Above the spatio-temporal scale of lobe complexes the morphology of the depositional element is less likely to be the result of autogenic processes acting on individual events and more likely to be controlled by allogenic factors, such as the interplay of basin subsidence and sediment supply (see stratigraphic interval scale of Sheets et al. 2002; Jobe et al. 2017) (Fig. 21). It should be noted that in confined basins established morphometric ranges for unconfined depositional element thicknesses break down due to variable degrees of confinement across systems (Prélat et al. 2010). The lobe-scale applicability of the model is therefore purely a hierarchical observation because lobe thicknesses will vary across systems.

Stratigraphic Position.—Lobe progradation is unlikely to be constant; fluctuations in sediment supply, relative sea level, or changes in routing may result in small-scale backstepping. This backstepping creates discrete boundaries between successive members in the Annot Basin (Callec 2004; Euzen et al. 2004) (Figs. 3, 5). These fluctuations will result in a non-uniform evolution of flow concentration during progradation, however on the basin-scale the overall trend of increasing flow concentration and subsequent onlap style will be maintained, with higher-density flows becoming more prevalent in the basin through progradation. These observations make the model most applicable to the early fill of confined deep-water systems, where confinement is greatest and distal thin-bedded turbidites will be most prevalent.

Low-density and thin-bedded turbidites also tend to form thinner successions than high-density and thick-bedded turbidites. This is because sediment volume and sedimentation rates are greater in higher-density flows and because differential compaction more heavily affects finer-grained successions. This has implications for the evolution of onlap because the distal lobe fringe will be thinner than the lobe axis. As a result, the intra-formational onlap against the underlying fringe will be much more difficult to detect through time as the draping low-density turbidites gradually become thinner as the basin fills, eventually resulting in the higher-density flows onlapping directly against the hemipelagic basin margin (Fig. 17). This relationship is seen in the Le Ray member (Fig. 6), where the thin-bedded fringe is gradually surmounted by later flows.

Other Variables.—This conceptual model aims to describe in simple terms the effect that autogenic flow evolution may have on onlap patterns in confined basins. Variables such as a waxing–waning sediment supply, hemipelagic aggradation rates, and the dominant grain size of the system are not discussed fully; however they will act to alter the autogenic processes that affect onlap and should be explored in future studies.

CONCLUSION

Understanding flow interaction with, and bed termination against, confining topography is critical for reconstructing the structural and sedimentological evolution of deep-water basins. This study presents a review of onlap styles in deep-water settings based on detailed field investigations and compares these results against those from a simple numerical model. Onlap terminations are shown to evolve in a predictable way through the progradation of a submarine lobe succession, with different lobe sub-environments identified at the basin margin through the migration of successive termination points and facies trends.

Initially termination points migrate towards the basin margins as low-density turbidites significantly drape the inherited basinal topography. Progressively higher-magnitude flows with greater sediment concentrations of the hybrid-bed-rich proximal fan fringe onlap these underlying deposits, causing the development of an intra-formational onlap surface that is characterized by either a basinward shift in termination points or a reduced distance between successive termination points towards the basin margin. Hybrid beds are also shown to constitute significant thicknesses of the proximal fringe in confined systems through long run-out transformation, slope-induced transformation, and intra-basinal slope instability. Progradation of the lobe off-axis over the proximal fringe will cause further intra-formational onlap as the lower-concentration off-axis deposits drape the slope. Onlap against the fringe drape will continue until it is surmounted and onlap occurs directly against the hemipelagic basin margin. Intra-formational onlap may also occur in the lobe axis through abrupt onlap of these high-concentration deposits against the underlying lower-concentration fringe or off-axis deposits.

These sedimentological processes act to modulate the allogenic signals present in the Grès d'Annot of the Annot Basin, with onlap patterns controlled by both allogenic processes, through tectonic deformation and

increasing sediment supply, and autogenic processes, through the interaction between longitudinal flow evolution and confining basin margins. Depositional hierarchy is also shown to be important when interpreting onlap patterns, with autogenic processes more important at the lobe scale and allogenic processes more important at the lobe-complex scale.

ACKNOWLEDGMENTS

Soutter is funded by Natural Environment Research Council (NERC) grant number NE/M00578X/1. Constructive reviews by B. Prather, Y. Spychala, and M. Mayall helped clarify both the content and presentation of the manuscript, and are gratefully acknowledged. Associate Editor S. Hubbard and Corresponding Editor J. Southard are thanked for editorial handling of the manuscript and additional comments. Stereonet 10 is acknowledged for data plotting.

REFERENCES

- AL JA'AJDI, O.S., McCAFFREY, W.D., AND KNELLER, B.C., 2004, Factors influencing the deposit geometry of experimental turbidity currents: implications for sand-body architecture in confined basins, *in* Lomas, S., and Joseph, P., eds., *Confined Turbidite Basins*: Geological Society of London, Special Publication 222, p. 45–58.
- AMY, L.A., McCAFFREY, W.D., AND KNELLER, B.C., 2004, The influence of a lateral basin-slope on the depositional patterns of natural and experimental turbidity currents, *in* Lomas, S., and Joseph, P., eds., *Deep-Water Sedimentation in the Alpine Basin of SE France: New Perspectives on the Grès d'Annot and Related Systems*: Geological Society of London, Special Publication 221, p. 311–330.
- APPS, G., 1987, *Evolution of the Grès d'Annot Basin, SW Alps* [Ph.D. thesis]: University of Liverpool, 434 p.
- APPS, G., PEEL, F., AND ELLIOTT, T., 2004, The structural setting and palaeogeographical evolution of the Grès d'Annot basin, *in* Lomas, S., and Joseph, P., eds., *Deep-Water Sedimentation in the Alpine Basin of SE France: New Perspectives on the Grès d'Annot and Related Systems*: Geological Society of London, Special Publication 221, p. 65–96.
- ARMITAGE, D.A., ROMANS, B.W., COVAULT, J.A., AND GRAHAM, S.A., 2009, The influence of mass-transport-deposit surface topography on the evolution of turbidite architecture: the Sierra Contreras, Tres Pasos Formation (Cretaceous), southern Chile: *Journal of Sedimentary Research*, v. 79, p. 287–301.
- AZIROZ-ZABALA, M., CARTIGNY, M.J., TALLING, P.J., PARSONS, D.R., SUMNER, E.J., CLARE, M.A., SIMMONS, S.M., COOPER, C., AND POPE, E.L., 2017, Newly recognized turbidity current structure can explain prolonged flushing of submarine canyons: *Science Advances*, v. 3, e1700200.
- BAAS, J.H., 2004, Conditions for formation of massive turbiditic sandstones by primary depositional processes: *Sedimentary Geology*, v. 166, p. 293–310.
- BAAS, J.H., BEST, J.L., AND PEAKALL, J., 2011, Depositional processes, bedform development and hybrid bed formation in rapidly decelerated cohesive (mud–sand) sediment flows: *Sedimentology*, v. 58, p. 1953–1987.
- BAKKE, K., KANE, I.A., MARTINSEN, O.J., PETERSEN, S.A., JOHANSEN, T.A., HUSTOFT, S., JACOBSEN, F.H., AND GROTH, A., 2013, Seismic modeling in the analysis of deep-water sandstone termination styles: *American Association of Petroleum Geologists, Bulletin*, v. 97, p. 1395–1419.
- BARKER, S.P., HAUGHTON, P.D.W., McCAFFREY, W.D., ARCHER, S.G., AND HAKES, B., 2008, Development of rheological heterogeneity in clay-rich high-density turbidity currents: Aptian Britannia Sandstone Member, UK continental shelf: *Journal of Sedimentary Research*, v. 78, p. 45–68.
- BEAUBOUËF, R.T., AND FRIEDMANN, S.J., 2000, High resolution seismic/sequence stratigraphic framework for the evolution of Pleistocene intra slope basins, western Gulf of Mexico: depositional models and reservoir analogs, *in* Weimer, P., Slatt, R.M., Coleman, J., Rossen, N.C., Nelson, H., Bouma, A.H., Styzen, M.J., and Lawrence, D.T., eds., *Deep-Water Reservoirs of the World: SEPM, Gulf Coast Section, 20th Annual Research Conference*, p. 40–60.
- BELL, D., KANE, I.A., PONTÉN, A.S., FLINT, S.S., HODGSON, D.M., AND BARRETT, B.J., 2018a, Spatial variability in depositional reservoir quality of deep-water channel-fill and lobe deposits: *Marine and Petroleum Geology*, v. 98, p. 97–115.
- BELL, D., STEVENSON, C.J., KANE, I.A., HODGSON, D.M., AND POYATOS-MORE, M., 2018b, Topographic controls on the development of contemporaneous but contrasting basin-floor depositional architectures: *Journal of Sedimentary Research*, v. 88, p. 1166–1189.
- BOULESTEIX, K., POYATOS-MORE, M., FLINT, S.S., TAYLOR, K., HODGSON, D.M., AND HASIOTIS, T.M., in press, Transport and deposition of mud in deep-water environments: processes and stratigraphic implications: *Sedimentology*.
- BOULESTEIX, K., POYATOS-MORE, M., FLINT, S., HODGSON, D.M., TAYLOR, K.G., AND PARRY, G.R., 2019, Sedimentary facies and stratigraphic architecture of deep-water mudstones beyond the basin-floor fan sandstone pinchout: <https://eartharxiv.org/3qrew/>.
- BOUMA, A.H., 1962, *Sedimentology of Some Flysch Deposits: A Graphic Approach to Facies Interpretation*: New York, Elsevier, 168 p.

- BRUNT, R.L., McCAFFREY, W.D., AND KNELLER, B.C., 2004, Experimental modeling of the spatial distribution of grain size developed in a fill-and-spill mini-basin setting: *Journal of Sedimentary Research*, v. 74, p. 438–446.
- CALLEC, Y., 2004, The turbidite fill of the Annot sub-basin (SE France): a sequence-stratigraphy approach, in Lomas, S., and Joseph, P., eds., *Deep-Water Sedimentation in the Alpine Basin of SE France: New Perspectives on the Grès d'Annot and Related Systems*: Geological Society of London, Special Publication 221, p. 111–135.
- CLARE, M.A., TALLING, P.J., CHALLENGOR, P., MALGESINI, G., AND HUNT, J., 2014, Distal turbidites reveal a common distribution for large (> 0.1 km³) submarine landslide recurrence: *Geology*, v. 42, p. 263–266.
- CLARK, J.D., AND STANBROOK, A., 2001, Formation of large-scale shear structures during deposition from high-density turbidity currents, Grès d'Annot Formation, south-east France: *Particulate Gravity Currents*, v. 31, p. 219–232.
- COVAULT, J.A., AND ROMANS, B.W., 2009, Growth patterns of deep-sea fans revisited: turbidite-system morphology in confined basins, examples from the California Borderland: *Marine Geology*, v. 265, p. 51–66.
- CUNHA, R.S., TINTERRI, R., AND MAGALHAES, P.M., 2017, Annot Sandstone in the Peira Cava basin: an example of an asymmetric facies distribution in a confined turbidite system (SE France): *Marine and Petroleum Geology*, v. 87, p. 60–79.
- DEPTUCK, M.E., PIPER, D.J., SAVOYE, B., AND GERVAIS, A., 2008, Dimensions and architecture of late Pleistocene submarine lobes off the northern margin of East Corsica: *Sedimentology*, v. 55, p. 869–898.
- DEVRIES, M., AND LINDHOLM, R.M., 1994, Internal architecture of a channel–levee complex, Cerro Toro Formation, Southern Chile, in Weimer, P., Bouma, A.H., and Perkins, B.F., eds., *Submarine Fans and Turbidite Systems: SEPM, Gulf Coast Section*, p. 105–114.
- DORRELL, R.M., PATACCI, M., AND McCAFFREY, W.D., 2019, Inflation of ponded, particulate-laden density currents: *Journal of Sedimentary Research*, v. 88, p. 1276–1282.
- DOUGHTY-JONES, G., MAYALL, M., AND LONERGAN, L., 2017, Stratigraphy, facies, and evolution of deep-water lobe complexes within a salt-controlled intraslope minibasin: *American Association of Petroleum Geologists, Bulletin*, v. 101, p. 1879–1904.
- DU FORNEL, E., JOSEPH, P., DESAUBLIAUX, G., ESCHARD, R., GUILLOCHEAU, F., LERAT, O., MULLER, C., RAVENNE, C., AND SZTRAKOS, K., 2004, The southern Grès d'Annot outcrops (French Alps): an attempt at regional correlation, in Lomas, S., and Joseph, P., eds., *Deep-Water Sedimentation in the Alpine Basin of SE France: New Perspectives on the Grès d'Annot and Related Systems*: Geological Society of London, Special Publication 221, p. 137–160.
- EGGENHUISEN, J.T., McCAFFREY, W.D., HAUGHTON, P.D., AND BUTLER, R.W., 2011, Shallow erosion beneath turbidity currents and its impact on the architectural development of turbidite sheet systems: *Sedimentology*, v. 58, p. 936–959.
- EGGENHUISEN, J.T., CARTIGNY, M.J., AND DE LEEUW, J., 2017, Physical theory for near-bed turbulent particle suspension capacity: *Earth Surface Dynamics*, v. 5, p. 269–281.
- ELLIOTT, T., APPS, G., DAVIES, H., EVANS, M., GHIBAUDO, G., AND GRAHAM, R.H., 1985, A structural and sedimentological traverse through the Tertiary foreland basin of the external Alps of south-east France, in Allen, P.A., and Homewood, P., eds., *Field Excursion Guidebook: International Association of Sedimentologists: Fribourg, Foreland Basins Conference*, p. 39–73.
- EUZEN, T., JOSEPH, P., DU FORNEL, E., LESUR, S., GRANJEON, D., AND GUILLOCHEAU, F., 2004, Three-dimensional stratigraphic modelling of the Grès d'Annot system, Eocene–Oligocene, SE France, in Lomas, S., and Joseph, P., eds., *Deep-Water Sedimentation in the Alpine Basin of SE France: New Perspectives on the Grès d'Annot and Related Systems*: Geological Society of London, Special Publication 221, p. 161–180.
- GARDINER, A.R., 2006, The variability of turbidite sandbody pinchout and its impact on hydrocarbon recovery in stratigraphically trapped fields, in Allen, M.R., Goffey, G.P., Morgan, R.K., and Walker, I.M., eds., *The Deliberate Search for the Stratigraphic Trap*: Geological Society of London, Special Publication 254, p. 267–287.
- GERVAIS, A., SAVOYE, B., PIPER, D.J., MULDER, T., CREMER, M., AND PICHEVIN, L., 2004, Present morphology and depositional architecture of a sandy confined submarine system: the Golo turbidite system (eastern margin of Corsica), in Lomas, S., and Joseph, P., eds., *Confined Turbidite Basins*: Geological Society of London, Special Publication 222, p. 59–89.
- GRECULA, M., FLINT, S., POTTS, G., WICKENS, D., AND JOHNSON, S., 2003, Partial ponding of turbidite systems in a basin with subtle growth-fold topography: Laingsburg–Karoo, South Africa: *Journal of Sedimentary Research*, v. 73, p. 603–620.
- GROENENBERG, R.M., HODGSON, D.M., PRELAT, A., LUTHI, S.M., AND FLINT, S.S., 2010, Flow-deposit interaction in submarine lobes: insights from outcrop observations and realizations of a process-based numerical model: *Journal of Sedimentary Research*, v. 80, p. 252–267.
- GRUNDTVAG, S.A., JOHANNESSEN, E.P., HELLAND-HANSEN, W., AND PLINK-BJØRKLUND, P., 2014, Depositional architecture and evolution of progradationally stacked lobe complexes in the Eocene Central Basin of Spitsbergen: *Sedimentology*, v. 61, p. 535–569.
- HANSEN, L.A.S., HODGSON, D.M., PONTÉN, A., BELL, D., AND FLINT, S., 2019, Quantification of basin-floor fan pinchouts: examples from the Karoo Basin, South Africa: *Frontiers in Earth Science*, v. 7, 12 p.
- HAUGHTON, P.D.W., 1994, Deposits of deflected and ponded turbidity currents, Sorbas basin, Southeast Spain: *Journal of Sedimentary Petrology*, v. 64, p. 233–246.
- HAUGHTON, P.D., 2000, Evolving turbidite systems on a deforming basin floor, Tabernas, SE Spain: *Sedimentology*, v. 47, p. 497–518.
- HAUGHTON, P.D., BARKER, S.P., AND McCAFFREY, W.D., 2003, “Linked” debrites in sand-rich turbidite systems: origin and significance: *Sedimentology*, v. 50, p. 459–482.
- HAUGHTON, P., DAVIS, C., McCAFFREY, W., AND BARKER, S., 2009, Hybrid sediment gravity flow deposits: classification, origin and significance: *Marine and Petroleum Geology*, v. 26, p. 1900–1918.
- HISCOTT, R.N., 1994, Loss of capacity, not competence, as the fundamental process governing deposition from turbidity currents: *Journal of Sedimentary Petrology*, v. 64, p. 209–214.
- HODGSON, N.A., FARNSWORTH, J., AND FRASER, A.J., 1992, Salt-related tectonics, sedimentation and hydrocarbon plays in the Central Graben, North Sea, UKCS, in Hardman, R.F.P., eds., *Exploration Britain: Geological Insights for the Next Decade*: Geological Society of London, Special Publication 67, p. 31–63.
- HODGSON, D.M., 2009, Distribution and origin of hybrid beds in sand-rich submarine fans of the Tanqua depocenter, Karoo Basin, South Africa: *Marine and Petroleum Geology*, v. 26, p. 1940–1956.
- HODGSON, D.M., AND HAUGHTON, P.D., 2004, Impact of syndepositional faulting on gravity current behaviour and deep-water stratigraphy: Tabernas–Sorbas Basin, SE Spain, in Lomas, S., and Joseph, P., eds., *Confined Turbidite Basins*: Geological Society of London, Special Publication 222, p. 135–158.
- HODGSON, D.M., FLINT, S.S., HODGETTS, D., DRINKWATER, N.J., JOHANNESSEN, E.P., AND LUTHI, S.M., 2006, Stratigraphic evolution of fine-grained submarine fan systems, Tanqua depocenter, Karoo Basin, South Africa: *Journal of Sedimentary Research*, v. 76, p. 20–40.
- FONNESU, M., HAUGHTON, P., FELLETTI, F., AND McCAFFREY, W., 2015, Short length-scale variability of hybrid event beds and its applied significance: *Marine and Petroleum Geology*, v. 67, p. 583–603.
- FONNESU, M., FELLETTI, F., HAUGHTON, P.D., PATACCI, M., AND McCAFFREY, W.D., 2018, Hybrid event bed character and distribution linked to turbidite system sub-environments: the North Apennine Gottero Sandstone (north-west Italy): *Sedimentology*, v. 65, p. 151–190.
- FORD, M., LICKORISH, W., AND KUSNIR, N., 1999, Tertiary foreland sedimentation in the southern subalpine chains, SE France: a geodynamic appraisal: *Basin Research*, v. 11, p. 315–336.
- KANE, I.A., AND PONTÉN, A.S., 2012, Submarine transitional flow deposits in the Paleogene Gulf of Mexico: *Geology*, v. 40, p. 1119–1122.
- KANE, I.A., McCAFFREY, W.D., AND MARTINSEN, O.J., 2009, Allogenic vs. autogenic controls on megafault formation: *Journal of Sedimentary Research*, v. 79, p. 643–651.
- KANE, I.A., CATTERALL, V., McCAFFREY, W.D., AND MARTINSEN, O.J., 2010, Submarine channel response to intrabasinal tectonics: the influence of lateral tilt: *American Association of Petroleum Geologists, Bulletin*, v. 94, p. 189–219.
- KANE, I.A., MCGEE, D.T., AND JOBE, Z.R., 2012, Halokinetic effects on submarine channel equilibrium profiles and implications for facies architecture: conceptual model illustrated with a case study from Magnolia Field, Gulf of Mexico, in Alsop, G.I. et al., eds., *Salt Tectonics, Sediment and Prospectivity*: Geological Society of London, Special Publication 363, p. 289–302.
- KANE, I.A., PONTÉN, A.S., VANGDAL, B., EGGENHUISEN, J.T., HODGSON, D.M., AND SPYCHALA, Y.T., 2017, The stratigraphic record and processes of turbidity current transformation across deep-marine lobes: *Sedimentology*, v. 64, p. 1236–1273.
- KILHAMS, B., HARTLEY, A., HUUSE, M., AND DAVIS, C., 2012, Characterizing the Paleocene turbidites of the North Sea: the Mey Sandstone Member, Lista Formation, UK Central Graben: *Petroleum Geoscience*, v. 18, p. 337–354.
- KNELLER, B.C., 1995, Beyond the turbidite paradigm: physical models for deposition of turbidites and their implications for reservoir prediction, in Hartley, A., and Prosser, D.J., eds., *Characterisation of Deep Marine Clastic Systems*: Geological Society of London, Special Publication 94, p. 29–46.
- KNELLER, B.C., AND McCAFFREY, W.D., 1995, Modelling the effects of salt-induced topography on deposition from turbidity currents: *SEPM, Gulf Coast Section*, p. 137–145.
- KNELLER, B.C., AND McCAFFREY, W.D., 1999, Depositional effects of flow non-uniformity and stratification within turbidity currents approaching a bounding slope: deflection, reflection and facies variation: *Journal of Sedimentary Research*, v. 69, p. 980–991.
- KNELLER, B.C., EDWARDS, D., McCAFFREY, W.D., AND MOORE, R., 1991, Oblique reflection of turbidity currents: *Geology*, v. 19, p. 250–252.
- KNELLER, B., DYKSTRA, M., FAIRWEATHER, L., AND MILANA, J.P., 2016, Mass-transport and slope accommodation: implications for turbidite sandstone reservoirs: *American Association of Petroleum Geologists, Bulletin*, v. 100, p. 213–235.
- KUBO, Y.S., 2004, Experimental and numerical study of topographic effects on deposition from two-dimensional, particle-driven density currents: *Sedimentary Geology*, v. 164, p. 311–326.
- JACKSON, C.A.-L., BARBER, G.P., AND MARTINSEN, O.J., 2008, Submarine slope morphology as a control on the development of sand-rich turbidite depositional systems: 3D seismic analysis of the Kyrre Fm (Upper Cretaceous), Måløy Slope, offshore Norway: *Marine and Petroleum Geology*, v. 25, p. 663–680.
- JACKSON, C.A.-L., ZAKARIA, A.A., JOHNSON, H.D., TONGKUL, F., AND CREVELLO, P.D., 2009, Sedimentology, stratigraphic occurrence and origin of linked debrites in the West Crocker Formation (Oligo-Miocene), Sabah, NW Borneo: *Marine and Petroleum Geology*, v. 26, p. 1957–1973.
- JOBE, Z.R., SYLVESTER, Z., HOWES, N., PIRMEZ, C., PARKER, A., CANTELLI, A., SMITH, R., WOLINSKY, M.A., O'BYRNE, C., SLOWEY, N., AND PRATHER, B., 2017, High-resolution, millennial-scale patterns of bed compensation on a sand-rich intraslope submarine fan, western Niger Delta slope: *Geological Society of America, Bulletin*, v. 129, p. 23–37.

- JOSEPH, P., AND LOMAS, S.A., 2004, Deep-water sedimentation in the Alpine Foreland Basin of SE France: new perspectives on the Grès d'Annot and related systems: an introduction: Geological Society, London, Special Publication 221, p. 1–16.
- LAMB, M.P., PARSONS, J.D., MULLENBACH, B.L., FINLAYSON, D.P., ORANGE, D.L., AND NITTROUER, C.A., 2008, Evidence for superelevation, channel incision, and formation of cyclic steps by turbidity currents in Eel Canyon, California: Geological Society of America, Bulletin, v. 120, p. 463–475.
- LEE, S.E., AMY, L.A., AND TALLING, P.J., 2004, The character and origin of thick base-of-slope sandstone units of the Peira Cava outlier, SE France, in Lomas, S., and Joseph, P., eds., Deep-Water Sedimentation in the Alpine Basin of SE France: New Perspectives on the Grès d'Annot and Related Systems: Geological Society of London, Special Publication 221, p. 331–347.
- LIU, Q., KNELLER, B., FALLGATTER, C., VALDEZ BUSO, V., AND MILANA, J.P., 2018, Tabularity of individual turbidite beds controlled by flow efficiency and degree of confinement: Sedimentology, v. 65, p. 2368–2387.
- LOMAS, S.A., AND JOSEPH, P., 2004, Confined turbidite systems, in Lomas, S., and Joseph, P., eds., Confined Turbidite Basins: Geological Society of London, Special Publication 222, p. 1–7.
- LOWE, D.R., 1982, Sediment gravity flows: II. Depositional models with special reference to the deposits of high-density turbidity currents: Journal of Sedimentary Petrology, v. 52, p. 279–297.
- LOWE, D.R., AND GUY, M., 2000, Slurry-flow deposits in the Britannia Formation (Lower Cretaceous), North Sea: a new perspective on the turbidity current and debris flow problem: Sedimentology, v. 47, p. 31–70.
- MARINI, M., MILLI, S., RAVNAS, R., AND MOSCATELLI, M., 2015, A comparative study of confined vs. semi-confined turbidite lobes from the Lower Messinian Laga Basin (Central Apennines, Italy): implications for assessment of reservoir architecture: Marine and Petroleum Geology, v. 63, p. 142–165.
- MARINI, M., PATACCI, M., FELLETTI, F., AND MCCAFFREY, W.D., 2016, Fill to spill stratigraphic evolution of a confined turbidite mini-basin succession, and its likely well bore expression: The Castagnola Fm, NW Italy: Marine and Petroleum Geology, v. 69, p. 94–111.
- MAYALL, M., LONERGAN, L., BOWMAN, A., JAMES, S., MILLS, K., PRIMMER, T., POPE, D., ROGERS, L., AND SKEENE, R., 2010, The response of turbidite slope channels to growth-induced seabed topography: American Association of Petroleum Geologists, Bulletin, v. 94, p. 1011–1030.
- MCCAFFREY, W.D., AND KNELLER, B.C., 2001, Process controls on the development of stratigraphic trap potential on the margins of confined turbidite systems and aids to reservoir evaluation: American Association of Petroleum Geologists, Bulletin, v. 85, p. 971–988.
- MCCAFFREY, W.D., AND KNELLER, B.C., 2004, Scale effects of non-uniformity on deposition from turbidity currents with reference to the Grès d'Annot of SE France, in Lomas, S., and Joseph, P., eds., Deep-Water Sedimentation in the Alpine Basin of SE France: New Perspectives on the Grès d'Annot and Related Systems: Geological Society of London, Special Publication 221, p. 301–310.
- MIDDLETON, G.V., AND HAMPTON, M.A., 1973, Sediment gravity flows: mechanics of flow and deposition, in Middleton, G.V., and Bouma, A.H., eds., Turbidites and Deep Water Sedimentation: Pacific Section, Society of Economic Paleontologists and Mineralogists, Book 2, Short Course Notes, p. 1–38.
- MOHRIG, D., AND BUTTLES, J., 2007, Deep turbidity currents in shallow channels: Geology, v. 35, p. 155–158.
- MOUGIN, F., 1978, Contribution à l'étude des Sédiments tertiaires de la partie orientale du synclinal d'Annot (Alpes de Haute Provence). Stratigraphie, Géochimie, Micropaléontologie [Unpublished Ph.D. Thesis]: Université Scientifique et Médicale de Grenoble, 165 p.
- MUCK, M.T., AND UNDERWOOD, M.B., 1990, Upslope flow of turbidity currents: a comparison among field observations, theory, and laboratory models: Geology, v. 18, p. 54–57.
- MULDER, T., AND ALEXANDER, J., 2001, The physical character of subaqueous sedimentary density flows and their deposits: Sedimentology, v. 48, p. 269–299.
- MUTTI, E., BERNOULLI, D., RICCI LUCCHI, F., AND TINTERRI, R., 2009, Turbidites and turbidity currents from Alpine "flysch" to the exploration of continental margins: Sedimentology, v. 56, p. 267–318.
- OLUBOVO, A.P., GAWTHORPE, R.L., BAKKE, K., AND HADLER-JACOBSEN, F., 2014, Salt tectonic controls on deep-water turbidite depositional systems: Miocene, southwestern Lower Congo Basin, offshore Angola: Basin Research, v. 26, p. 597–620.
- ORTIZ-KARPE, A., HODGSON, D.M., AND MCCAFFREY, W.D., 2015, The role of mass-transport complexes in controlling channel avulsion and the subsequent sediment dispersal patterns on an active margin: the Magdalena Fan, offshore Colombia: Marine and Petroleum Geology, v. 64, p. 58–75.
- ORTIZ-KARPE, A., HODGSON, D.M., JACKSON, C.A.-L., AND MCCAFFREY, W.D., 2016, Mass-transport complexes as markers of deep-water fold-and-thrust belt evolution: insights from the southern Magdalena Fan, Offshore Colombia: Basin Research, v. 30, p. 65–88.
- PATACCI, M., HAUGHTON, P.D., AND MCCAFFREY, W.D., 2014, Rheological complexity in sediment gravity flows forced to decelerate against a confining slope, Braux, SE France: Journal of Sedimentary Research, v. 84, p. 270–277.
- PICKERING, K.T., AND HISCOTT, R.N., 1985, Contained (reflected) turbidity currents from the Middle Ordovician Cloridorme Formation, Quebec, Canada: an alternative to the antidune hypothesis: Sedimentology, v. 32, p. 373–394.
- PINTER, P.R., BUTLER, R.W., HARTLEY, A.J., MANISCALCO, R., BALDASSINI, N., AND DI STEFANO, A., 2017, Tracking sand-fairways through a deformed turbidite system: the Numidian (Miocene) of Central Sicily, Italy: Basin Research, v. 30, p. 480–501.
- PIPER, D.J., COCHONAT, P., AND MORRISON, M.L., 1999, The sequence of events around the epicentre of the 1929 Grand Banks earthquake: initiation of debris flows and turbidity current inferred from sidescan sonar: Sedimentology, v. 46, p. 79–97.
- PRATHER, B.E., O'BYRNE, C., PIRMEZ, C., AND SYLVESTER, Z., 2017, Sediment partitioning, continental slopes and base-of-slope systems: Basin Research, v. 29, p. 394–416.
- PRATHER, B.E., BOOTH, J.R., STEFFENS, G.S., AND CRAIG, P.A., 1998, Classification, lithologic calibration, and stratigraphic succession of seismic facies of intraslope basins, deep-water Gulf of Mexico: American Association of Petroleum Geologists, Bulletin, v. 82, p. 701–728.
- PRATHER, B.E., PIRMEZ, C., AND WINKER, C.D., 2012, Stratigraphy of linked intraslope basins: Brazos–Trinity system western Gulf of Mexico, in Prather B.E. et al., eds., Application of the Principles of Seismic Geomorphology to Continental-Slope and Base-of-Slope Systems: Case Studies from Seafloor and Near-Seafloor Analogues: SEPM, Special Publication 99, p. 83–109.
- PRÉLAT, A., HODGSON, D.M., AND FLINT, S.S., 2009, Evolution, architecture and hierarchy of distributary deep-water deposits: a high-resolution outcrop investigation from the Permian Karoo Basin, South Africa: Sedimentology, v. 56, p. 2132–2154.
- PRÉLAT, A., COVAULT, J.A., HODGSON, D.M., FILDANI, A., AND FLINT, S.S., 2010, Intrinsic controls on the range of volumes, morphologies, and dimensions of submarine lobes: Sedimentary Geology, v. 232, p. 66–76.
- PUIGDEFABREGAS, C., GJELBERG, J.M., AND VAKSDAL, M., 2004, The Grès d'Annot in the Annot syncline: outer basin-margin onlap and associated soft-sediment deformation, in Lomas, S., and Joseph, P., eds., Deep-Water Sedimentation in the Alpine Basin of SE France: New Perspectives on the Grès d'Annot and Related Systems: Geological Society of London, Special Publication 221, p. 367–388.
- RAVENNE, C., RICHE, P., TREMOIERES, P., AND VIALLY, R., 1987, Sédimentation et tectonique dans le bassin marin Eocène supérieur-Oligocène des Alpes du Sud: Revue de l'Institut Français du Pétrole, v. 42, p. 529–553.
- SALLES, L., FORD, M., JOSEPH, P., DE VESLUZ, C.L.C., AND LE SOLLEUZ, A., 2011, Migration of a synclinal depocenter from turbidite growth strata: the Annot syncline, SE France: Bulletin de la Société Géologique de France, v. 182, p. 199–220.
- SALLES, L., FORD, M., AND JOSEPH, P., 2014, Characteristics of axially-sourced turbidite sedimentation on an active wedge-top basin (Annot Sandstone, SE France): Marine and Petroleum Geology, v. 56, p. 305–323.
- SHEETS, B.A., HICKSON, T.A., AND PAOLA, C., 2002, Assembling the stratigraphic record: depositional patterns and time-scales in an experimental alluvial basin: Basin Research, v. 14, p. 287–301.
- SINCLAIR, H.D., 1994, The influence of lateral basin slopes on turbidite sedimentation in the Annot Sandstones of SE France: Journal of Sedimentary Petrology, v. 64, p. 42–54.
- SINCLAIR, H.D., 1997, Tectonostratigraphic model for underfilled peripheral foreland basins: an Alpine perspective: Geological Society of America, Bulletin, v. 109, p. 324–346.
- SINCLAIR, H.D., 2000, Delta-fed turbidites infilling topographically complex basins: a new depositional model for the Annot Sandstones, SE France: Journal of Sedimentary Research, v. 70, p. 504–519.
- SINCLAIR, H.D., AND TOMASSO, M., 2002, Depositional evolution of confined turbidite basins: Journal of Sedimentary Research, v. 72, p. 451–456.
- SOMME, T.O., PIPER, D.J., DEPTUCK, M.E., AND HELLAND-HANSEN, W., 2011, Linking onshore-offshore sediment dispersal in the Golo source-to-sink system (Corsica, France) during the late Quaternary: Journal of Sedimentary Research, v. 81, p. 118–137.
- SOUTHERN, S.J., PATACCI, M., FELLETTI, F., AND MCCAFFREY, W.D., 2015, Influence of flow containment and substrate entrainment upon sandy hybrid event beds containing a co-genetic mud-clast-rich division: Sedimentary Geology, p. 321, p. 105–122.
- SOUTTER, E.L., KANE, I.A., AND HUISE, M., 2018, Giant submarine landslide triggered by Palaeocene mantle plume activity in the North Atlantic: Geology, v. 46, p. 511–514.
- STANBROOK, D.A., AND CLARK, J.D., 2004, The Marnes Brunes Inférieures in the Grand Coyer remnant: characteristics, structure and relationship to the Grès d'Annot, in Lomas, S., and Joseph, P., eds., Deep-Water Sedimentation in the Alpine Basin of SE France: New Perspectives on the Grès d'Annot and Related Systems: Geological Society of London, Special Publication 221, v. 285–300.
- STANLEY, D.J., 1980, The Saint-Antonin conglomerate in the Maritime Alps: a model for coarse sedimentation on a submarine slope: Smithsonian Contributions to the Marine Sciences, v. 5, p. 1–25.
- STANLEY, D.J., AND MUTTI, E., 1968, Sedimentological evidence for an emerged land mass in the Ligurian sea during the Palaeogene: Nature, v. 218, 32 p.
- SMITH, R.U., 2004a, Silled sub-basins to connected tortuous corridors: sediment distribution systems on topographically complex sub-aqueous slopes, in Lomas, S., and Joseph, P., eds., Confined Turbidite Basins: Geological Society of London, Special Publication 222, p. 23–43.
- SMITH, R., 2004b, Turbidite systems influenced by structurally induced topography in the multi-sourced Welsh Basin, in Lomas, S., and Joseph, P., eds., Confined Turbidite Basins: Geological Society of London, Special Publication 222, p. 209–228.
- SMITH, R., AND JOSEPH, P., 2004, Onlap stratal architectures in the Grès d'Annot: geometric models and controlling factors, in Lomas, S., and Joseph, P., eds., Deep-Water Sedimentation in the Alpine Basin of SE France: New Perspectives on the Grès d'Annot

- and Related Systems: Geological Society of London, Special Publication 221, p. 389–399.
- SPYCHALA, Y.T., HODGSON, D.M., FLINT, S.S., AND MOUNTNEY, N.P., 2015, Constraining the sedimentology and stratigraphy of submarine intraslope lobe deposits using exhumed examples from the Karoo Basin, South Africa: *Sedimentary Geology*, v. 322, p. 67–81.
- SPYCHALA, Y.T., HODGSON, D.M., STEVENSON, C.J., AND FLINT, S.S., 2016, Aggradational lobe fringes: the influence of subtle intrabasinal seabed topography on sediment gravity flow processes and lobe stacking patterns: *Sedimentology*, v. 64, p. 582–608.
- SPYCHALA, Y.T., HODGSON, D.M., PRÉLAT, A., KANE, I.A., FLINT, S.S., AND MOUNTNEY, N.P., 2017, Frontal and lateral submarine lobe fringes: comparing sedimentary facies, architecture, and flow processes: *Journal of Sedimentary Research*, v. 87, p. 75–96.
- SPYCHALA, Y., EGGENHUISEN, J., TILSTON, M., AND POHL, F., 2019, The influence of basin settings and flow properties on the dimensions of submarine lobe elements: <https://eartharxiv.org/sk8v3/>.
- STEVENSON, C.J., JACKSON, C.A.-L., HODGSON, D.M., HUBBARD, S.M., AND EGGENHUISEN, J.T., 2015, Deep-water sediment bypass: *Journal of Sedimentary Research*, v. 85, p. 1058–1081.
- STEVENSON, C.J., FELDEN, P., GEORGIPOULOU, A., SCHÖNKE, M., KRÄSTEL, S., PIPER, D.J., LINDHORST, K., AND MOSHER, D., 2018, Reconstructing the sediment concentration of a giant submarine gravity flow: *Nature Communications*, v. 9, 2616.
- STRAUB, K.M., MOHRIG, D., MCELROY, B., BUTTLES, J., AND PIRMEZ, C., 2008, Interactions between turbidity currents and topography in aggrading sinuous submarine channels: a laboratory study: *GSA Bulletin*, v. 120, p. 368–385.
- SYLVESTER, Z., CANTELLI, A., AND PIRMEZ, C., 2015, Stratigraphic evolution of intraslope minibasins: insights from surface-based model: *American Association of Petroleum Geologists, Bulletin*, v. 99, p. 1099–1129.
- SYMONS, W.O., SUMNER, E.J., PAULL, C.K., CARTIGNY, M.J., XU, J.P., MAIER, K.L., LORENSEN, T.D., AND TALLING, P.J., 2017, A new model for turbidity current behavior based on integration of flow monitoring and precision coring in a submarine canyon: *Geology*, v. 45, p. 367–370.
- TALLING, P.J., AMY, L.A., AND WYNN, R.B., 2007, New insight into the evolution of large-volume turbidity currents: comparison of turbidite shape and previous modelling results: *Sedimentology*, v. 54, p. 737–769.
- TINTERRI, R., MAGALHAES, P.M., TAGLIAFERRI, A., AND CUNHA, R.S., 2016, Convolute laminations and load structures in turbidites as indicators of flow reflections and decelerations against bounding slopes. Examples from the Marnoso–arenacea Formation (northern Italy) and Annot Sandstones (south eastern France): *Sedimentary Geology*, v. 344, p. 382–407.
- TÓKÉS, L., AND PATACCI, M., 2018, Quantifying tabularity of turbidite beds and its relationship to the inferred degree of basin confinement: *Marine and Petroleum Geology*, v. 97, p. 659–671.
- TOMASSO, M., AND SINCLAIR, H.D., 2004, Deep-water sedimentation on an evolving fault-block: the Braux and St Benoit outcrops of the Grès d’Annot, in Lomas, S., and Joseph, P., eds., *Deep-Water Sedimentation in the Alpine Basin of SE France: New Perspectives on the Grès d’Annot and Related Systems*: Geological Society of London, Special Publication 221, p. 267–283.
- WALTHER, J., 1894, Einleitung in die Geologie als historische Wissenschaft, in *Lithogenesis der Gegenwart*: Jena, G. Fischer, v. 3, p. 535–1055.
- WEIMER, P., AND LINK, M.H., 1991, Global petroleum occurrences in submarine fans and turbidite systems, in Weimer P., and Link M.H., eds., *Seismic Facies and Sedimentary Processes of Submarine Fans and Turbidite Systems*: *Frontiers in Sedimentary Geology*, New York, Springer, p. 9–67.
- WILSON, D., DAVIES, J.R., WATERS, R.A., AND ZALASIEWICZ, J.A., 1992, A fault-controlled depositional model for the Aberystwyth Grits turbidite system: *Geological Magazine*, v. 129, p. 595–607.
- WYNN, R.B., MASSON, D.G., STOW, D.A., AND WEAVER, P.P., 2000, The Northwest African slope apron: a modern analogue for deep-water systems with complex seafloor topography: *Marine and Petroleum Geology*, v. 17, p. 253–265.

Received 11 December 2018; accepted 7 June 2019.